p-wave pion production from nucleon-nucleon collisions

V. Baru,[1,2] E. Epelbaum,[1,3] J. Haidenbauer,[1,4] C. Hanhart,[1,4] A. E. Kudryavtsev,[2] V. Lensky,[2,5] and U.-G. Meißner[1,3,4]

[1]*Institut für Kernphysik (Theorie) and Jülich Center for Hadron Physics, Forschungszentrum Jülich GmbH, D-52425 Jülich, Germany*

[2]*Institute for Theoretical and Experimental Physics, 117218, B. Cheremushkinskaya 25, Moscow, Russia*

[3]*Helmholtz-Institut für Strahlen- und Kernphysik (Theorie), Bethe Center for Theoretical Physics, Universität Bonn, D-53115 Bonn, Germany*

[4]*Institute for Advanced Simulation, Forschungszentrum Jülich GmbH, D-52425 Jülich, Germany*

[5]*European Centre for Theoretical Studies in Nuclear Physics and Related Areas (ECT*), Strada delle Tabarelle 286, Villazzano (Trento), I-38050 TN, Italy*

(Received 30 July 2009; published 19 October 2009)

We investigate p-wave pion production in nucleon-nucleon collisions up to next-to-next-to-leading order in chiral effective field theory. In particular, we show that it is possible to describe simultaneously the p-wave amplitudes in the $pn \to pp\pi^-$, $pp \to pn\pi^+$, $pp \to d\pi^+$ channels by adjusting a single low-energy constant accompanying the short-range operator that is available at this order. This study provides a nontrivial test of the applicability of chiral effective field theory to reactions of the type $NN \to NN\pi$.

DOI: 10.1103/PhysRevC.80.044003 PACS number(s): 12.39.Fe, 25.10.+s, 13.60.Le, 21.30.Fe

I. INTRODUCTION

With the advent of chiral perturbation theory (ChPT), the low-energy effective field theory (EFT) of QCD, high-accuracy calculations for hadronic reactions with a controlled error estimation have become possible [1,2]. In that framework, $\pi\pi$- [3] and πN-scattering [4] observables and nuclear forces [5] are calculated based on a perturbative expansion in q/Λ_χ with q referring to either a generic momentum of external particles or the pion mass m_π, and $\Lambda_\chi \sim 1$ GeV being the chiral symmetry breaking scale. An extension of this scheme to pion production in nucleon-nucleon (NN) collisions turned out to be considerably more difficult. A straightforward application of the power counting proposed by Weinberg [6,7] to the reactions $NN \to NN\pi$ [8,9] failed badly (see also Ref. [10] where it was pointed out that the naive power counting using the heavy baryon formalism is not applicable above the pion production threshold). Indeed, for neutral pion production in pp collisions, the corrections due to the next-to-leading order (NLO) increased the discrepancy with the data and, moreover, the next-to-next-to-leading order (NNLO) contributions turned out to be even larger than the NLO terms [11]. The origin of these difficulties was identified quite early by Cohen *et al.* [12] (see also Ref. [13]), who stressed that the additional new scale, inherent in reactions of the type $NN \to NN\pi$, needs to be accounted for in the power counting. Because the two nucleons in the initial state need to have sufficiently high kinetic energy to produce the on-shell pion in the final state, the initial center-of-mass momentum needs to be larger than

$$p_{\rm thr} = \sqrt{M_N\, m_\pi}\,, \quad \text{with} \quad \frac{p_{\rm thr}}{\Lambda_\chi} \simeq 0.4\,, \tag{1}$$

where m_π and M_N refer to the the pion and nucleon mass, respectively. The proper way to include this scale was presented in Ref. [14] and implemented in Ref. [15]; see Ref. [16] for a review article. As a result, pion p-wave production is governed by the tree-level diagrams up to NNLO in the modified power counting scheme of Ref. [14]. However, for pion s-wave production, pion loops start to contribute already at NLO. It was demonstrated in Ref. [17] that all irreducible loop contributions at NLO cancel altogether, and the net effect of going to NLO was shown to increase the most important operator for charged pion production, first investigated in Ref. [18], by a factor of 4/3. This was sufficient to overcome the apparent discrepancy with the data in that channel. But the neutral pion channel is more challenging—it still calls for a calculation of subleading loop contributions. First steps in this direction were taken in Refs. [19]. We further emphasize that the $\Delta(1232)$ isobar should be taken into account explicitly as a dynamical degree of freedom [12] because the Δ-nucleon mass difference, ΔM, is also of the order of $p_{\rm thr}$. This general argument was confirmed numerically in phenomenological calculations [20–22].

Pion p-wave production in NN collisions receives an important contribution from the leading $(\bar{N}N)^2\pi$ contact term in the effective Lagrangian, which also figures importantly in the three-nucleon force [14,23]. In addition, the same operator also contributes to the processes $\gamma d \to \pi NN$ [24,25] and $\pi d \to \gamma NN$ [26,27], as well as to weak reactions such as, e.g., tritium β decay and proton-proton (pp) fusion [28,29], as visualized in Fig. 1. Note that this operator appears in the above reactions in very different kinematics, ranging from very low energies for both incoming and outgoing NN pairs in pd scattering and the weak reactions up to relatively high initial energies for the NN induced pion production. In Ref. [30] it was shown that both the ^{3}H and ^{3}He binding energies and the triton β decay can be described with the same contact term. However, an apparent discrepancy between the strength of the contact term needed in $pp \to pn\pi^+$ and in $pp \to de^+\nu_e$ was reported in Ref. [31]. If the latter observation were true, it would certainly question the applicability of chiral EFT to the reactions $NN \to NN\pi$.

To better understand the discrepancy reported in Ref. [31], in this article we simultaneously analyze different pion production channels. In particular, we calculate the p-wave amplitudes for the reactions $pn \to pp\pi^-$, $pp \to pn\pi^+$, and $pp \to d\pi^+$. Note that even in these channels the contact term

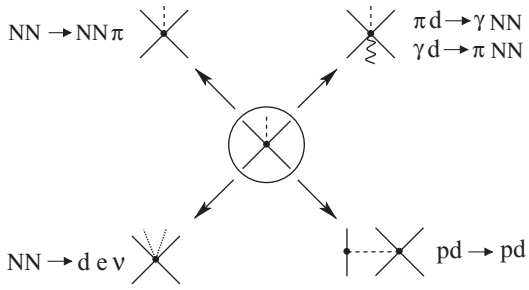

FIG. 1. Illustration of the various reactions, where the leading $(N\bar{N})^2\pi$ contact term contributes.

occurs in entirely different dynamical regimes. For the first channel p-wave pion production goes along with the slowly moving protons in the $^1S_0$ final state, whereas for the other two channels the $^1S_0$ pp state is to be evaluated at the relatively large initial momentum. Notwithstanding, all three channels of the reaction $NN \to NN\pi$ seem to give consistent results for the low-energy constant (LEC) d that represents the strength of the contact term, as we will show in the present article. We discuss which additional data are needed to further support this conclusion. We argue that the origin of the discrepancy reported in Ref. [31] is not due to the different kinematics of $NN \to NN\pi$ and pp fusion but rather in the inconsistency in the partial-wave amplitudes used in the analysis. In addition, we also comment on technical issues related to the work of Ref. [31].

Our manuscript is organized as follows: In Sec. II we discuss the general features and the relevant observables for p-wave pion production. In Sec. III the power counting is outlined with special emphasis on the p-wave amplitudes. Our results for the various pion production channels are presented in Sec. IV. Here, we also discuss the role of the leading πN-scattering parameters, c_3 and c_4, for the p-wave pion production amplitudes. We close with a short summary.

II. GENERAL REMARKS

It is not obvious, *a priori*, that with just a single contact term, which contributes to the various reactions shown in Fig. 1, a consistent description of all these channels can be achieved. The purpose of the contact term is twofold: it should, on the one hand, absorb any sensitivities to the employed NN wave functions and in this way remove the model dependence in the evaluation of the observables. On the other hand, it provides a parametrization of the short-range physics that contributes to the process being considered. Thus, the strength of the contact term is necessarily dependent on the method applied to regularize the integrals (typically a cutoff) and also on the NN interaction that is used for generating the wave functions.

For the case at hand the contact term connects $NN\,S$ waves in the initial state with $NN\,S$ waves in the final state. Because the contact term is a local four-nucleon operator, after including the NN distortions its contribution scales as the product of the initial and final NN wave functions at the origin. Each of these wave functions, in turn, may be represented by the inverse of the corresponding Jost function [32]. The reason why it is expected to be possible that the same contact term can be used in all reactions listed above is that the energy dependence of the Jost function is fixed by the on-shell NN data and is therefore independent of the unknown short-range physics. Specifically, the NN distortions can be represented as an integral over the relevant phase shifts by means of the so-called Omnès function [33]—see also the discussion in Ref. [34]. This is correct up to contributions from the left-hand cuts and the high-energy behavior of the NN interaction; both are expected to be of higher order in the expansion. As opposed to the energy dependence, the overall scale of the distortions can be shown to be sensitive to things like the NN interaction and the cutoff employed [35]. Clearly, what needs to be assumed in the argument given is that there is a proper separation of scales in the problem. Note that the expansion parameter $p_{\rm thr}/\Lambda_\chi \sim 0.4$ is quite large. In this sense a consistent description of all mentioned reactions with the same contact term provides a nontrivial test of the applicability of the chiral expansion to pion production in NN collisions.

One might ask why we take the effort of this study, because in Ref. [31] it was already shown that a consistent description is not possible. The answer is twofold: first, we found that the partial-wave decomposition of Ref. [36], the result of which was used in Ref. [31], is not correct (see Sec. IV C). This is why we decided to directly compare to the data in the present work. Second, there is also a conceptual problem in the work of Ref. [31]: as was outlined above, as long as different phase-equivalent NN interactions are used, it should be possible to absorb the model dependence of the calculation in a single counterterm up to higher-order corrections. However, in Ref. [31] pion production from initial NN and $N\Delta$ states is not treated on equal footing. Rather, the contribution from the Δ isobar excitation is added on top of and independent of the employed NN interactions. Thus, it is quite possible that the utilized $NN \to N\Delta$ transition potential is too strong. Specifically, it is not constrained by the empirical NN phase shifts as is the case when considering the NN and $N\Delta$ amplitudes consistently within a coupled-channels (Lippmann-Schwinger-like) scattering equation [20]. In this sense, it should not come as a surprise that it was not possible to absorb the model dependencies in a single counterterm within the scheme used in Ref. [31]. To avoid this problem, in this work we employ the coupled-channels NN model of Ref. [37] that involves the $NN \to N\Delta$ transition potential.

Eventually all reactions shown in Fig. 1 should be analyzed consistently. This would, however, require a calculation to third order in the chiral expansion of the process $\gamma d \to \pi NN$ and $\pi d \to \gamma NN$ or a rather involved three-nucleon calculation for the tritium β decay that goes beyond the scope of this work. Instead, as a next step in this ambitious program, we analyze here in detail various pion production channels. Note that although these reactions appear to have similar kinematics, the relevant transition for the reaction $pn \to pp\pi^-$ involves very low momenta in the NN $^1S_0$ state and considerably higher momenta ($\sim p_{\rm thr}$) in the $^3S_1$ channel while the situation is just opposite for the reactions $pp \to (d/pn)\pi^+$. Thus, a simultaneous description of these reaction with a single short-range operator indeed provides a highly nontrivial consistency test of our approach. Note further that the $(N\bar{N})^2\pi$ short-range

operator we are interested in here does not contribute to the $pp \to pp\pi^0$ transition that is, therefore, not considered in the present work. Thus, the only reactions of interest for this study are $pp \to (pn/d)\pi^+$ and $pn \to pp\pi^-$. Here the relevant transitions are ${}^1S_0 \to {}^3S_1 p$ for the former and $({}^3S_1 - {}^3D_1) \to {}^1S_0 p$ for the latter, where the small letter labels the pion angular momentum. Because the main focus of this work is on the role of the contact term, we will concentrate on observables where the final NN system is in an S wave, which largely simplifies the numerical work. However, as outlined below, the contribution of NN P waves to observables might be relevant for the reaction $pp \to pn\pi^+$. This potential problem renders this channel not very convenient for the extraction of the counterterm, as will be discussed in Sec. IV.

To be specific, we calculate in this work the differential cross sections and analyzing powers for the reactions $pp \to d\pi^+$, $pp \to pn\pi^+$, and $pn \to (pp)_{^1S_0}\pi^-$. Here the symbol $(pp)_{^1S_0}$ indicates that in the corresponding measurement the final pp relative momentum was restricted kinematically to be less than 38 MeV/c ($M_{pp} - 2M_N \leqslant 1.5$ MeV) that leads to a projection on the ${}^1S_0$ pp final state. For all the mentioned observables experimental data are available or will be available soon in the energy range of relevance here. In addition to the anisotropy of the pion angular distributions, all observables are sensitive to both s- and p-wave pion production. Although there exists an NLO calculation for s-wave pion production in $pp \to d\pi^+$ using ChPT, its theoretical uncertainty is still sizable [17]. For s-wave pion production accompanied by a transition of an isospin-1 NN pair to an isospin-1 NN pair (e.g., in $pp \to pp\pi^0$), no sufficiently accurate ChPT calculation is available at present. Because we focus here on the p-wave amplitudes, we extract the s-wave amplitudes directly from the data to minimize the uncertainties of our calculation. The phase of these amplitudes is then imposed using the Watson theorem [32]; see the discussion in Sec. IV.

It is well known that p-wave pion production in $pp \to d\pi^+$ and in $pp \to pn\pi^+$ is strongly dominated by the transition ${}^1D_2 \to {}^3S_1 p$ due to a strong coupling of the initial NN state to the ${}^5S_2$ $N\Delta$ state [38]. Therefore, the amplitude we are interested in has only a minor impact on the observables. In other words, the uncertainty for the extraction of the counterterm from these reactions will be significant. The situation is much more promising for the reaction $pn \to pp\pi^-$: here the amplitude of interest is the leading p wave. In addition, the strength of the s-wave amplitude can be taken from the reaction $pp \to pp\pi^0$ using isospin symmetry and correcting for the final-state interaction (FSI) as discussed in Sec. IV D. Unfortunately, no data are presently available for $pn \to pp\pi^-$ at sufficiently low energies. Nevertheless, as will be shown below, already the higher-energy data provide some insights. In addition, data at lower excess energies will be available soon [39].

The goal of the present investigation is to explore whether it is possible to obtain a simultaneous description of all $NN \to NN\pi$ channels. A more quantitative study including a statistical analysis of the data and an estimation of the theoretical uncertainty is postponed until accurate experimental data will become available for $pn \to pp\pi^-$ at low energies.

III. FORMALISM

Our calculations are based on the effective chiral Lagrangian with explicit Δ degrees of freedom. The leading πN and $\pi N\Delta$ interaction terms read [40,41]

$$\mathcal{L}^{(0)} = N^\dagger \left[\frac{1}{4f_\pi^2} \boldsymbol{\tau} \cdot (\dot{\boldsymbol{\pi}} \times \boldsymbol{\pi}) + \frac{g_A}{2f_\pi} \boldsymbol{\tau} \cdot \vec{\sigma} \cdot \vec{\nabla} \boldsymbol{\pi} \right] N + \frac{h_A}{2f_\pi} [N^\dagger (\boldsymbol{T} \cdot \vec{S} \cdot \vec{\nabla} \boldsymbol{\pi}) \Psi_\Delta + \text{h.c.}] + \cdots \quad (2)$$

while the first corrections have the form

$$\mathcal{L}^{(1)} = \frac{1}{8M_N f_\pi^2} [i N^\dagger \boldsymbol{\tau} \cdot (\boldsymbol{\pi} \times \vec{\nabla} \boldsymbol{\pi}) \cdot \vec{\nabla} N + \text{h.c.}] - \frac{1}{f_\pi^2} N^\dagger \left[c_3 (\vec{\nabla} \boldsymbol{\pi})^2 + \frac{1}{2} \left(c_4 + \frac{1}{4M_N} \right) \times \varepsilon_{ijk} \varepsilon_{abc} \sigma_k \tau_c \partial_i \pi_a \partial_j \pi_b \right] N - \frac{d}{f_\pi} N^\dagger (\boldsymbol{\tau} \cdot \vec{\sigma} \cdot \vec{\nabla} \boldsymbol{\pi}) N \, N^\dagger N + \cdots . \quad (3)$$

The ellipses stand for further terms that are not relevant for the present study. In the equations above f_π denotes the pion decay constant in the chiral limit, g_A is the axial-vector coupling of the nucleon, h_A is the $\Delta N\pi$ coupling, N and Ψ_Δ correspond to the nucleon and Δ fields, respectively, and $\vec{S}$ and $\boldsymbol{T}$ are the transition spin and isospin matrices, normalized according to:

$$S_i S_j^\dagger = \tfrac{1}{3}(2\delta_{ij} - i\epsilon_{ijk}\sigma_k) \qquad T_i T_j^\dagger = \tfrac{1}{3}(2\delta_{ij} - i\epsilon_{ijk}\tau_k). \quad (4)$$

We also emphasize that the effective Lagrangian of Ref. [40] contains another $(\bar{N}N)^2\pi$ contact operator that can be shown to be redundant as a consequence of the Pauli principle [14,23,28].

We are now in the position to discuss the relevant scales and counting rules for p-wave pion production. We assign the outgoing two-nucleon relative momentum p' and the outgoing pion momentum k_π to be of order of m_π and introduce the expansion parameter

$$\chi \simeq \frac{k_\pi}{p} \simeq \frac{p'}{p} \simeq \frac{m_\pi}{p} \simeq \frac{p}{M_N} \simeq \frac{\Delta M}{M_N}, \quad (5)$$

where $p \simeq p_{\text{thr}}$ is the initial two-nucleon relative momentum. The counting rules for the time-dependent vertices, such as, e.g., the Weinberg-Tomosawa (WT) vertex in $\mathcal{L}^{(0)}$, are discussed in detail in Refs. [17,42]. At leading order one finds that the WT vertex is $\propto 2\omega_\pi$ with ω_π being the energy of the outgoing (on-shell) pion. The diagrams contributing to the production operator at LO and at NLO are shown in Fig. 2,

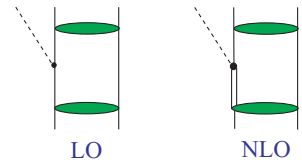

FIG. 2. (Color online) Leading and next-to-leading diagrams for the p-wave amplitudes of $NN \to NN\pi$. Single (double) solid lines denote nucleons (Δs), dashed lines denote pions, and green ellipses correspond to the NN wave functions in the initial and final states.

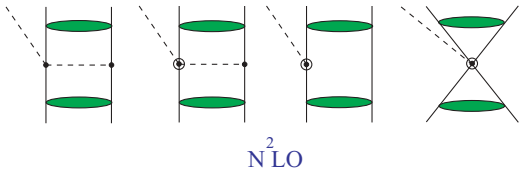

FIG. 3. (Color online) Diagrams that contribute at NNLO to the p-wave amplitudes of $NN \to NN\pi$. Subleading vertices are marked as $\odot$.

whereas the corresponding graphs at NNLO are depicted in Fig. 3. At NLO there are only diagrams in which the pion is produced through the excitation of the Δ resonance. The relative suppression of these diagrams as compared to the ones involving the nucleon is accounted for by the Δ propagator that is suppressed by $1/p$ as compared to $1/m_\pi$ in the nucleon case. To see that the diagrams in Fig. 3 indeed contribute at NNLO for p-wave pion production consider, as an example, the first graph in this figure. Its contribution can be estimated using dimensional analysis as follows:

$$\frac{\omega_\pi}{f_\pi^2}\frac{1}{p^2}\frac{k_\pi}{f_\pi} \simeq \frac{1}{f_\pi^3}\frac{k_\pi}{m_\pi}\frac{m_\pi}{M_N}. \tag{6}$$

Here we used that the outgoing pion momentum k_π enters the πNN vertex to allow for the p-wave amplitude. To understand the suppression factor this operator should be compared with the LO contribution $k_\pi/(f_\pi^3 m_\pi)$. Thus, one gets an order χ^2 suppression for the first diagram of Fig. 3. Similarly, using the $\pi\pi NN$ vertex from $\mathcal{L}^{(1)}$ in combination with the p/f_π scaling for the πNN vertex one arrives again at a χ^2 suppression for the second diagram in Fig. 3. Further details can be found in Appendix A that contains explicit expressions for the diagrams shown in Figs. 2 and 3. Once the amplitudes are evaluated they need to be convoluted with proper NN wave functions. Ideally, one would use wave functions derived from the same formalism, namely ChPT. However, up to now these are only available for energies below the pion production threshold [5]. We therefore use the so-called hybrid approach, first introduced by Weinberg [7], based on the transition operators derived within the effective field theory and convoluted with realistic wave functions [37]. This procedure should also provide reasonable results; however, a reliable uncertainty estimate is possible only at the level of the transition operator.

IV. RESULTS AND DISCUSSION

A. Parameters of the calculation

To the order we are working, the following low-energy constants (LECs) appear in the calculation: f_π, g_A, h_A, c_3, c_4, and d. Only the last LEC cannot be taken from other sources, for its value strongly depends on the NN wave functions employed. We adopt the following values of the parameters: $f_\pi = 92.4$ MeV, $g_A = 1.32$, $h_A \simeq 2.1 g_A = 2.77$, $c_3 = -0.79$ GeV^{-1}, and $c_4 = 1.33$ GeV^{-1}. The values of the LECs c_3 and c_4 are taken from Ref. [43]. From the fit to πN threshold parameters, two solutions for the c_i are given in Ref. [43] corresponding to the different choices of h_A ($h_A \simeq 2.1 g_A$ and $h_A \simeq 2.1$). The sensitivity of the results to the different values of c_3 and c_4 will be also discussed. As already mentioned in the Introduction, the power counting scheme calls for a dynamical treatment of the Δ isobar as a result of the comparable numerical value of the Δ-nucleon mass difference and $p_{\rm thr}$. The implications of integrating out the Δ degrees of freedom for the processes at hand are discussed in Appendix B.

The deuteron wave function and the NN-scattering amplitudes used in the calculation are generated from the CCF NN potential [37]. As described above, we do not calculate the s-wave pion amplitudes in this work but rather take both their strength and the phases directly from experiment. To be specific, for the reaction $pn \to pp\pi^-$ we aim at the description of the double differential cross sections and the analyzing power measured at TRIUMF [44,45] and PSI [46]. Following the Watson theorem to parametrize the relevant ${}^3P_0 \to {}^1S_0 s$ amplitude, we use the ansatz $\tilde{C} e^{i\delta_{^3P_0}} \Psi^{(+)}_{p'}(r=0)$, where the inverse Jost function in the ${}^1S_0$ partial wave, $\Psi^{(+)}_{p'}(r=0)$, and the initial phase shift $\delta_{^3P_0}$ are calculated from the NN model used, and the parameter $\tilde{C}$ is fitted to reproduce the corresponding amplitude extracted from the TRIUMF data using a partial-wave analysis [45,47]. It is interesting to note that the ${}^3P_0 \to {}^1S_0 s$ amplitude from the TRIUMF analysis at[1] $\eta = 0.66$ ($T_{\rm lab} = 353$ MeV) is about 25% larger than that extracted from the $pp \to pp\pi^0$ measurement at CELSIUS [48]. A similar inconsistency is discussed in Ref. [49], where it is argued that the total cross sections at low energies for $pp \to pp\pi^0$ recently measured at COSY are about 50% larger than those at CELSIUS and IUCF as a result of the missing acceptance at small angles for both CELSIUS and IUCF.

For the reaction $pp \to d\pi^+$ the s-wave amplitude occurs in the ${}^3P_1 \to {}^3S_1 s$ partial wave and can be related to the total cross section at threshold. The most precise way of getting this quantity is to extract it from the width of pionic deuterium atom, measured at PSI with high accuracy [50,51]. This procedure gives the following value of α, the total cross section divided by η : $\alpha = 252^{+5}_{-11}$ μb [52]. Thus, we adjust the magnitude of the ${}^3P_1 \to {}^3S_1 s$ amplitude to be in agreement with this observable.

As mentioned above the value of d depends on the NN interaction employed and on the method used to regularize the overlap integrals. Indeed, in Refs. [14,28] a strong sensitivity of the LEC d to the regulator is reported. It therefore does not make much sense to compare values for d as found in different calculations. What makes sense, however, is to compare results on the level of observables and this is what we will do below. We will adjust the value of d in such a way to get the best simultaneous qualitative description of all channels of $NN\pi$.

[1] Traditionally, the energy in the pion production reactions is given in terms of η, the (maximum) pion momentum allowed in units of the pion mass.

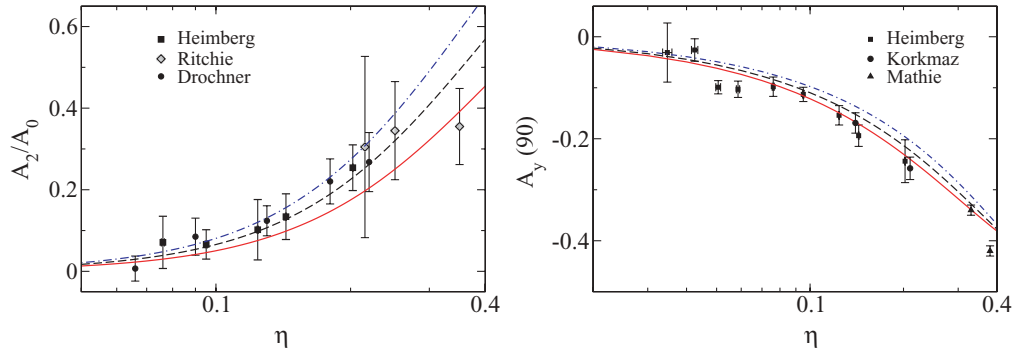

FIG. 4. (Color online) Results for A_2/A_0 [see Eq. (7)] (left panel) and the analyzing power at 90° (right panel) for the reaction $pp \to d\pi^+$ for different values for the strength of d [in units $1/(f_\pi^2 M_N)$]. Shown are $d = 3$ (red solid line), $d = 0$ (black dashed line), and $d = -3$ (blue dot-dashed line). The data are from Refs. [53–57]. The strength and phase of the s-wave amplitude is fixed from data.

B. Reaction $pp \to d\pi^+$

We begin with a discussion of the results for the reaction $pp \to d\pi^+$. In Fig. 4, we compare our calculation for various values of d with the experimentally available angular asymmetry parameter A_2/A_0. The coefficients A_i are related to the unpolarized differential cross section via

$$\frac{d\sigma}{d\Omega} = A_0 + A_2 P_2(\cos\theta_\pi) \tag{7}$$

with $P_2(x)$ being the second Legendre polynomial and θ_π the pion angle in the center-of-mass frame. We also show results for the analyzing power at 90°. In both cases the observables are plotted as functions of the parameter η. Here and in what follows, the value of the LEC d is always given in units $1/(f_\pi^2 M_N)$. Notice that at low energies, it is sufficient to just show the analyzing power at 90° because its angular dependence is proportional to $\sin\theta_\pi$. To illustrate this we also present in Fig. 5 the analyzing power as a function of the scattering angle for two different energies $\eta = 0.14$ and $\eta = 0.21$. At $\eta \simeq 0.5$ the angular dependence of the analyzing power starts to deviate significantly from $\sin\theta_\pi$ due to the onset of d waves. Clearly, at these (and higher) energies we cannot expect our calculation to agree with the data anymore. As can be seen from the figures, the data at small η, especially the analyzing power, prefers a positive value for d; our fit resulted in $d = 3$ for the best value. To demonstrate the effect of the LEC d on the observables, in Fig. 5 and in subsequent figures we also give the results with $d = 0$ and with the negative LEC $d = -3$.

C. Reaction $pn \to pp\pi^-$

We now turn to the reaction $pn \to pp\pi^-$. As it was explained in Sec. II, for this reaction channel the relevant pion p wave occurs in conjunction with the two-nucleon pair in the $^1S_0$ state. It is known experimentally that in the isospin-1 channel the final P-wave diproton contributions (Pp and Ps) start growing with the energy rather rapidly so that already for excess energies around 30 MeV they provide about 50% of the total cross section [48]. Therefore, to be sensitive to our particular amplitude one needs to isolate experimentally the S-wave diproton state by putting kinematical cuts on the two-nucleon relative momentum. This is exactly what was done in the experimental study of $pn \to pp\pi^-$ at TRIUMF [44,45]. In particular, they measured the differential cross section $d^2\sigma/(d\Omega dm_{pp}^2)$ and analyzing power A_y for $T_{\rm lab} = 353$ MeV ($\eta = 0.66$), where the final diproton relative momentum p' was restricted to be not larger than 38 MeV/c ($M_{pp} - 2M_N \simeq 1.5$ MeV). A similar measurement for the analyzing power was also performed at PSI [46] for $T_{\rm lab} = 345$ MeV and pp invariant masses $M_{pp} - 2M_N < 6$ MeV. It is interesting to note that the positions of the peaks in A_y seem to differ somewhat in these experiments (see Fig. 6), although the data of Ref. [46] have much larger uncertainties than those of Ref. [44]. Unfortunately, presently data for $pn \to pp\pi^-$ are available only at such high energies where our corresponding results in the $pp \to d\pi^+$ channel already start to deviate considerably from the experiment. Therefore, for the reaction $pn \to pp\pi^-$ we expect likewise only a qualitative description.

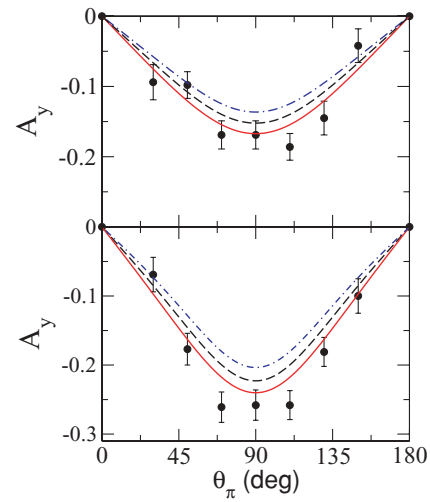

FIG. 5. (Color online) Results for the analyzing power at $\eta = 0.14$ (upper panel) and $\eta = 0.21$ (lower panel) as functions of the angle θ_π for the reaction $pp \to d\pi^+$ for different values of d. Shown are $d = 3$ (red solid line), $d = 0$ (black dashed line), and $d = -3$ (blue dot-dashed line). The data are from Ref. [56]. The strength and phase of the s-wave amplitude is fixed from data.

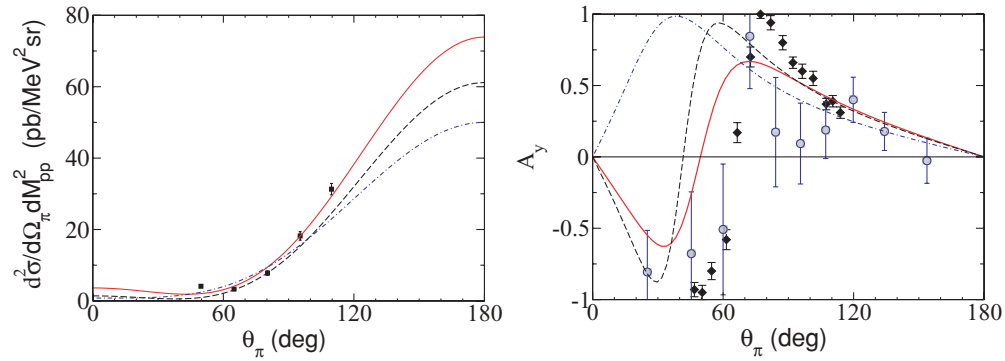

FIG. 6. (Color online) Results for $d^2\sigma/d\Omega_\pi dM_{pp}^2$ (left panel) and A_y (right panel) for $pn \to pp(^1S_0)\pi^-$. Shown are the results for $d = 3$ (red solid line), $d = 0$ (black dashed line), and $d = -3$ (blue dot-dashed line). The data are from TRIUMF [44,45] (black squares) and from PSI [46] (blue circles).

Nevertheless, a comparison with the experimental data in this channel is also quite instructive and shows a preference for a positive value of d as visualized in Fig. 6. Fortunately, there will soon be a measurement for the same observables at lower energies at COSY [39]. Once these data will be available we should be able to draw more quantitative conclusions on the value of the parameter d needed for the reaction $pn \to pp\pi^-$.

D. Reaction $pp \to pn\pi^+$

The reaction $pp \to pn\pi^+$ is the most difficult and the least convenient one for the extraction of the contact term. In addition to the fact that here, as in $pp \to d\pi^+$, pion p-wave production is mainly driven by the $^1D_2$ initial state, in addition NN P waves contribute for isospin-1 as well as for isospin-zero NN final states. At the energies considered in the experimental investigation, $\eta = 0.22$, 0.42, and 0.5, the Pp amplitudes may contribute significantly [48,58,59]. They should be particularly important in view of the smallness of the $^1S_0$ amplitude—even small contributions to A_2, see Eqs. (7) and (9), can affect the partial-wave analysis considerably. In the partial-wave analysis performed in Ref. [36], these Pp contributions were not taken into account at all. Also there are contributions to A_0 from the isospin-1 NN final states that potentially increase the uncertainty of the analysis, especially in view of the differences in the experimental results in $pp \to pp\pi^0$ as already discussed above. These arguments alone cast serious concerns on the partial-wave analysis performed in Ref. [36]. But there is an even more direct evidence of problems with the extraction of the partial-wave amplitudes of Ref. [36] that we now discuss in detail. The observables measured for the reaction $\vec{p}p \to pn\pi^+$ in Ref. [36] include the coefficients A_0 and A_2 in the differential cross section, see Eq. (7) and the analyzing power $A_y(90^\circ)$. Neglecting the Pp contributions these observables can be expressed in terms of the three partial-wave amplitudes with the isospin-zero pn-state $a_0(^1S_0 \to {}^3S_1 p)$ (the single amplitude, where the $(N\bar{N})^2\pi$ contact term contributes), $a_1(^3P_1 \to {}^3S_1 s)$, and $a_2(^1D_2 \to {}^3S_1 p)$ and the contribution of the isospin-1 channel denoted as $A_0^{I=1}$ via

$$A_0 = \frac{|a_0|^2 + |a_1|^2 + |a_2|^2}{4} + A_0^{I=1}, \quad (8)$$

$$A_2 = \frac{|a_2|^2}{4} - \frac{1}{\sqrt{2}}\mathrm{Re}[a_0 a_2^*], \quad (9)$$

$$A_y(90^\circ)\left(A_0 - \frac{A_2}{2}\right) = \frac{1}{4}(\sqrt{2}\mathrm{Im}[a_1 a_0^*] + \mathrm{Im}[a_1 a_2^*]), \quad (10)$$

where $(A_0 - A_2/2)$ is just $d\sigma/d\Omega(90^\circ)$ from Eq. (7). Using the system of Eqs. (8)– (10) one can determine the amplitudes a_0, a_1, and a_2 provided one knows the isospin-1 piece $A_0^{I=1}$. The latter was extracted in Ref. [36] from the measurement of the total cross section in the reaction $pp \to pp\pi^0$ reported in Ref. [60]. However, the FSI in the $pp \to pp\pi^0$ reaction is very different to that in the $pp \to pn\pi^+$ channel. To estimate the difference note that in the energy region studied, which is less than 20 MeV, the dominant partial wave is the one where the final two-nucleon state is in the S wave. In this case the correction factor would be proportional to the ratio of the inverse Jost functions squared integrated over the phase space

$$R = \frac{\int d^3p' k_\pi |F_{pn}(p')|^2}{\int d^3p' k_\pi |F_{pp}^{\mathrm{CC}}(p')|^2}, \quad (11)$$

where $F_{pn}(p')$ and $F_{pp}^{\mathrm{CC}}(p')$ are the inverse Jost functions for the pn and pp $^1S_0$ states, respectively. As discussed above, although the Jost function itself depends on the NN model used, its energy dependence does not. We may, therefore, evaluate R using any sensible model for the NN interaction. For a separable NN potential there exists an analytic expression for the Jost function in the pp system in the presence of the Coulomb interaction [61,62]. Using it one finds that the ratio R is about 1.5 for $\eta = 0.22$ and about 1.2 for $\eta = 0.42$. Similar results are obtained using the CCF NN interaction [37]. Thus, compared to the original analysis performed in Ref. [36], the isospin-1 contribution at $\eta = 0.22$ should be enhanced by more than a factor of two if, in addition, one utilizes the new, larger experimental data from COSY for the total cross section for $pp \to pp\pi^0$ [49]. This change, of course, will significantly affect the results of the partial-wave analysis. Given the above difficulties with the partial-wave analysis of Ref. [36], we decided to compare our results directly to the experimentally measured quantities. Aiming presently at a

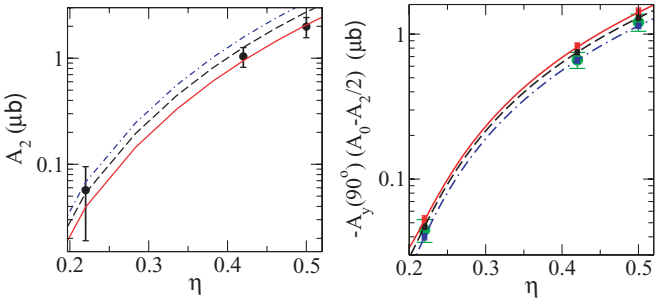

FIG. 7. (Color online) Results for the magnitude of A_2 (left panel) and $A_y(90^\circ)(A_0 - A_2/2)$ (right panel) for the reaction $pp \to pn\pi^+$ for different values of the contact term. The notation of curves is the same as in Fig. 4. The data are from Ref. [36].

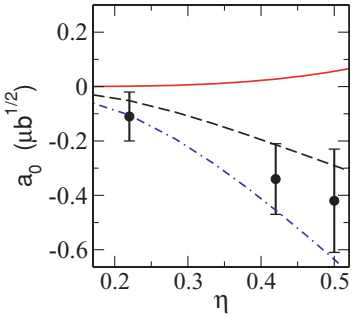

FIG. 8. (Color online) Comparison of a_0 as it results from our analysis in comparison to the partial-wave amplitude extracted in Ref. [36]. The notation of curves is the same as in Fig. 4. Because our calculations well describe all observables of Ref. [36], this figure nicely illustrates the problem of the partial-wave decomposition of this reference.

qualitative description of the data, we will not include the Pp states in this work.

The results of our calculation for A_2 are shown in Fig. 7. Again, positive values of the contact term with $d \sim 3$ seem to be preferred. We emphasize, however, that these results should be treated with care because the calculations at higher energies can be affected by P-wave contributions, whereas the lowest point is not very sensitive to the value of d due to the large experimental uncertainty. We can also check whether our results are consistent with the measurement of the analyzing power that is related to our amplitudes via Eq. (10). To allow for this comparison, however, we need to know the pion s-wave amplitude a_1. At present, this quantity is known theoretically only up-to-and-including terms at NLO. Therefore, to minimize the uncertainty of the current study, we extract this amplitude directly from data on the total cross section in $pp \to pn\pi^+$ through Eq. (8). We employ the amplitude $A_0^{I=1}$ consistent with the data at COSY and correct for the FSI factor as described above and take the amplitudes a_0 and a_2 from our NNLO calculation. In the right panel of Fig. 7 we compare our results for $A_y(90^\circ)(A_0 - A_2/2)$ with the corresponding data. Because we use the experimental total cross sections to extract a_1, our results, given by red ($d = 3$), black ($d = 0$), and blue ($d = -3$) squares in the right panel of Fig. 7, can be presented at specific energies only. The squares include the experimental uncertainty in the total cross section A_0 used to extract a_1. To guide the eye, we also show the results of interpolations between the three energies. It is seen that the magnitude $A_y(90^\circ)(A_0 - A_2/2)$ is much less sensitive to the value of the LEC d than, e.g., A_2. Note further that the experimental points do not include a 12% uncertainty due to systematic errors in A_0 and A_2.

Because we do not know the contribution of the $NN\,P$ waves to the $pp \to pn\pi^+$ observables at present, and an improved partial-wave analysis would require a careful study of various uncertainties, we do not try to extract a_0 from the data. However, to illustrate the potential effect of the changes discussed above (up to $NN\,P$ waves) on a_0, in Fig. 8 we show the results of our calculation for a_0 in comparison to the old extraction of Ref. [36]. Evidently, although all data presented in Ref. [36] are in a good agreement with our calculation (as demonstrated in Fig. 7), the partial-wave amplitude is not at all described; see the solid curve for our results with $d = 3$ in Fig. 8, which illustrates clearly that the partial-wave solution given in Ref. [36] should be abandoned. It is interesting to note that in Ref. [31] it was stressed that a positive value for a_0 is necessary to achieve a result for pion production that is consistent with the ones for the weak rates. This is in accord with our findings based solely on the data for $NN \to NN\pi$. Here we do not aim at a more quantitative comparison with Ref. [31], because of the technicalities discussed in the beginning of Sec. II.

Finally, we would like to discuss the sensitivity of our results to the parameters c_i. As shown in Appendix A, for the ${}^1S_0 \to {}^3S_1$ or ${}^3S_1 \to {}^1S_0$ NN transitions the parameters c_i occur in the combination $C_i^{{}^3S_1} = c_3/2 + c_4 + 1/(4M_N)$. This combination appears to be largely constrained by the πN data because the different sets of c_i from the recent analysis [43] give basically the same value for $C_i^{{}^3S_1}$. In addition, to the order we are working at, this combination is fully absorbed in the counterterm because the corresponding potential for $NN \to NN\pi$, see the second diagram in Fig. 3, is just a constant up to higher-order terms

$$V^{c_i}_{{}^1S_0,{}^3S_1} \sim C_i^{{}^3S_1} \frac{(\vec{p} - \vec{p}\,')^2}{(\vec{p} - \vec{p}\,')^2 + m_\pi^2} = C_i^{{}^3S_1}[1 + \mathcal{O}(\chi^2)]. \qquad (12)$$

Due to a coupled-channels effect, the same combination of c_i also contributes in the ${}^3D_1 \to {}^3S_1 \to {}^1S_0 p$ partial wave. The situation is different when D waves contribute at the level of the transition operator. The combinations of c_i in the ${}^3D_1 \to {}^1S_0 p$ amplitude for $pn \to pp\pi^-$ and in the ${}^1D_2 \to {}^3S_1 p$ amplitude for $pp \to (d/pn)\pi^+$ will influence the observables, for at the order we are working at there is no contact term that can absorb the resulting dependence on the LECs c_i. It is worth mentioning that the combinations of c_i in these partial waves are constrained only weakly by πN data. In particular, the combination of c_i in the ${}^3D_1$ partial wave, $C_i^{{}^3D_1} = c_3 - c_4 - 1/(4M_N)$, changes from 2 to 7 depending on which of the sets of c_i given in Ref. [43] is used. Thus, we conclude that the reaction $NN \to NN\pi$ may serve as an additional source of information to constrain the c_i's, complementary to the πN [43,63] and NN [64] data (see, however, Ref. [65] for some criticism). However, for a more quantitative study of

the constraints implied by pion production, and by πN- and NN-scattering data, a more complete and consistent analysis is necessary, which we postpone to a future work.

V. SUMMARY AND OUTLOOK

We performed a calculation of p-wave pion production amplitudes in NN collisions in three different channels ($pn \to pp\pi^-$, $pp \to d\pi^+$, and $pp \to pn\pi^+$) in the framework of chiral effective field theory. The relevant partial-wave transition that depends on the $(N\bar{N})^2\pi$ low-energy constant d is ${}^3S_1 \to {}^1S_0 p$ for the first channel and ${}^1S_0 \to {}^3S_1 p$ for the others. Therefore, it is clear that the study of different channels of the pion production reaction $NN \to NN\pi$ probes the corresponding operator in very different kinematical regimes and, thus, provides a nontrivial test for the validity of the employed approach. Our analysis of all the three channels resulted in values for the LEC d that are consistent with each other. In addition, we also point out an inconsistency in the partial-wave analysis for $pp \to pn\pi^+$ carried out in Ref. [36]. Our findings can be interpreted as an indication that the source of the discrepancy reported in Ref. [31] is not due to the difference in the kinematics between $NN \to NN\pi$ and tritium β decay but rather caused by the inconsistency in the partial-wave analysis for $pp \to pn\pi^+$ as well as by some technicalities with respect to the work of Ref. [31] that we also discussed in our article.

Our investigation implies that calculations within effective field theory yield reliable results for pion production in NN collisions utilizing the same value for d even though the corresponding contact term enters at very different kinematics in the reactions $pn \to pp\pi^-$, $pp \to d\pi^+$, and $pp \to pn\pi^+$. To confirm this conjecture, (i) one needs to reanalyze the reaction $pp \to pn\pi^+$ using the complete experimental information available for $pp \to pp\pi^0$ as input and (ii) one needs new data for the process $pn \to pp\pi^-$ at lower energies. We would like to stress that the near-threshold measurement of the reaction $pn \to (pp)_{^1S_0}\pi^-$, where $(pp)_{^1S_0}$ signifies that the final pp state is constrained to be in the S wave by a kinematical cut, is the cleanest way to extract information on the contact term from pion production processes. Such measurements are already under way at COSY. Indeed, in the near future both $pp \to (pp)_{^1S_0}\pi^0$ and $pn \to (pp)_{^1S_0}\pi^-$ will be measured even with polarized initial state [39]. In addition, a consistent calculation for both tritium β decay as well as low-energy pd scattering should be performed. We plan to perform these calculations in the future.

ACKNOWLEDGMENTS

We thank S. Nakamura for useful discussions related to the results of his work. The work of E.E. and V.B. was supported in parts by funds provided from the Helmholtz Association to the young investigator group "Few-Nucleon Systems in Chiral Effective Field Theory" (Grant VH-NG-222). This research is part of the EU HadronPhysics2 project "Study of Strongly Interacting Matter" under the Seventh Framework Programme of EU (Grant 227431). Work supported in part by DFG (SFB/TR 16, "Subnuclear Structure of Matter"), by the DFG-RFBR Grant (436 RUS 113/991/0-1) and by the Helmholtz Association through funds provided to the virtual institute "Spin and Strong QCD" (VH-VI-231). V.B., A.K., and V.L. acknowledge the support of the Federal Agency of Atomic Research of the Russian Federation. V.L. and A.K. acknowledge the hospitality of the Institute für Kernphysik at FZ Jülich.

APPENDIX A: REACTION AMPLITUDES

In this Appendix we present expressions for the matrix elements for the reactions we consider. To calculate them, we used the technique developed in Ref. [66].

1. General considerations

Let us consider pionic reactions involving the NN system, for example $NN \to NN\pi$, $\pi d \to NN$, and so on. In the most general case, an amplitude corresponding to the matrix element of a particular production and/or absorption operator between states with given initial (j, l, s) and final (j', l', s') total angular momentum of a nucleon pair, its orbital momentum and total spin[2] is written as

$$\mathcal{A}^{\text{full}}[jls, j'l's'] = \mathcal{A}^{\text{tree}}[jls, j'l's'] + \mathcal{A}^{\text{FSI}}[jls, j'l's'] + \mathcal{A}^{\text{ISI}}[jls, j'l's'] + \mathcal{A}^{\text{ISI+FSI}}[jls, j'l's'], \tag{A1}$$

where "tree" stands for the tree production amplitude, i.e., where there is no NN (or $N\Delta$) interaction both in the initial and in the final state, and FSI, ISI, ISI + FSI refer to the amplitudes with final state, initial state, and both final- and initial-state interaction included, in order. In this equation we imply that the spin-angular part (as well as the isospin part) of the amplitudes are factored out. Note that because there is a third particle that carries angular momentum, the pion, the total angular momentum j of the initial two-nucleon state can differ from that of the final two-nucleon state, j'. Obviously, the total angular momentum of the final particles has to be equal to that of the initial ones. Given the tree amplitude as a function of the initial p and final p' relative momenta, $\mathcal{A}^{\text{tree}}[jls, j'l's'](p, p')$, the remaining amplitudes are given by the following formulas:

$$\mathcal{A}^{\text{FSI}}[jls, j'l's'] = \sum_{l'',s''} \int \frac{d^3q}{(2\pi)^3} \frac{\mathcal{A}^{\text{tree}}[jls, j'l''s''](p, q)\, \mathcal{M}[j', l''s'', ls](q, p')}{4M_{1'}M_{2'}[q^2/(2\mu_{1'2'}) - E' - i0]}, \tag{A2}$$

[2]To unambiguously specify the partial wave, the pion angular momentum should, in general, also be given. We, however, omit it because it is only the p-wave pion production that is considered here.

$$\mathcal{A}^{\rm ISI}[jls,\, j'l's'] = \sum_{l'',s''} \int \frac{d^3q}{(2\pi)^3} \frac{\mathcal{M}[j, ls, l''s''](p,q)\, \mathcal{A}^{\rm tree}[jl''s'',\, j'l's'](q,\, p')}{4M_1M_2[q^2/(2\mu_{12}) - E - i0]}, \tag{A3}$$

$$\mathcal{A}^{\rm ISI+FSI}[jls,\, j'l's'] = \sum_{l'',s''} \sum_{l''',s'''} \int \frac{d^3q}{(2\pi)^3} \frac{d^3\ell}{(2\pi)^3} \frac{\mathcal{M}[j, ls, l''s''](p,q)\, \mathcal{A}^{\rm tree}[jl''s'',\, j'l'''s'''](q,\ell)\, \mathcal{M}[j', l'''s''', l's'](\ell,\, p')}{4M_1M_2\big[q^2/(2\mu_{12}) - E - i0\big] \times 4M_{1'}M_{2'}\big[\,\ell^2/(2\mu_{1'2'}) - E' - i0\big]}, \tag{A4}$$

where $M_{1,2}(M_{1',2'})$ are the masses of the particles in the intermediate state that are related via the NN interaction to the initial (final) state, $\mu_{12}(\mu_{1'2'})$ are the corresponding reduced masses, $E(E')$ is the energy of the initial (final) two-nucleon state in its center-of-mass frame, $\mathcal{M}[j, l_i s_i, l_f s_f]$ is the NN half–off-shell $\mathcal{M}$ matrix corresponding to a transition from the state (jl_is_i) to the state (jl_fs_f), and the sums are over all the intermediate states with given j, j', l, l', s, and s'. We use the following relation between the $\mathcal{M}$ matrix and the commonly used $\mathcal{T}$ matrix: $\mathcal{M} = -8\pi^2\sqrt{M_1M_2M_3M_4}\mathcal{T}$, where the M_i are the masses of interacting particles.

The formulas given above also hold for the case when there is a transition through an intermediate $N\Delta$ state going to a final (from an initial) state via an NN-$N\Delta$ interaction. In this case the $NN\,\mathcal{M}$ matrices have to be replaced by the appropriate NN-$N\Delta$ matrices, and the propagators entering Eqs. (A2)–(A4) that correspond to the $N\Delta$ intermediate state have to be modified according to

$$\frac{1}{4M_1M_2[q^2/(2\mu_{12}) - E - i0]} \longrightarrow \frac{1}{4\sqrt{2}M_1M_2[q^2/(2\mu_{12}) - (E - \Delta M) - i0]}, \tag{A5}$$

where ΔM is the nucleon-Δ mass difference (note also the factor $1/\sqrt{2}$). Of course, a tree diagram with a $N\Delta$ initial or final state gives a nonzero contribution only when it is inserted as a building block into those of FSI and ISI diagrams that have $N\Delta$ as an intermediate state.

In case of a deuteron in the final state, the corresponding $\mathcal{M}$ matrices should be replaced by the deuteron wave functions according to

$$\mathcal{A}^{\rm FSI}[jls,\, 1] = \frac{1}{\sqrt{2M_N}} \sum_{l''} \int \frac{d^3q}{(2\pi)^3}\, \mathcal{A}^{\rm tree}[jls,\, 1l''s''](p,q) i^{l''} \psi^{l''}(q), \tag{A6}$$

where $\psi^{l''}(q)$ are the deuteron wave functions corresponding to the angular momentum l'', normalized by the condition

$$\int \frac{d^3q}{(2\pi)^3} \{[\psi^0(q)]^2 + [\psi^2(q)]^2\} = 1. \tag{A7}$$

Thus, the two-nucleon propagator for the deuteron in the final state is absorbed in the wave functions and the normalization has changed. Analogous expressions can be written down for the deuteron in the initial state and also for the deuteron in the initial and final states. Note that in the case of the deuteron in the inital and/or final state the tree diagrams appear only as building blocks for the calculation of the ISI/FSI and ISI + FSI diagrams according to Eqs. (A2)–(A4) and (A6), respectively. They do not contribute independently because then there are no free nucleons in the initial and/or final state.

2. The reaction $pn \to pp\pi^-$

Here and below we use the spectroscopic notation ${}^{2S+1}L_J$ for the NN and $N\Delta$ partial waves rather than the $[jls]$ notation used in the previous section. The transitions that contribute to the reaction $pn \to pp\pi^-$ at energies close to threshold are ${}^3S_1 \to {}^1S_0p$, ${}^3D_1 \to {}^1S_0p$ in the isospin-zero initial state, and ${}^3P_0 \to {}^1S_0s$ in the isospin-1 initial state. The spin-angular structure of the amplitude reads

$$\mathcal{M}_{pn\to pp\pi^-} = \big\{A_1(\vec{\mathcal{S}}\hat{p}) + C_1(\vec{\mathcal{S}}\hat{k}_\pi) + C_2\,\vec{\mathcal{S}}\big[(\hat{p}\hat{k}_\pi)\hat{p} - \tfrac{1}{3}\hat{k}_\pi\big]\big\}\mathcal{I}'^{\dagger}, \tag{A8}$$

where $\vec{\mathcal{S}} = \chi_2^T \frac{\sigma_2}{\sqrt{2}}\vec{\sigma}\chi_1$, $\mathcal{I}' = \chi_{2'}^T \frac{\sigma_2}{\sqrt{2}}\chi_{1'}$ denote normalized spin structures corresponding to the initial spin-triplet and final spin-singlet states, in order. Here and below, $\hat{p}$, $\hat{p}\,'$, $\hat{k}_\pi$ denote unit vectors of initial and final relative momenta of two nucleons and that of the pion momentum, respectively, and the χ's with corresponding indices stand for the spinors of the initial and final nucleons. In turn, A_1, C_1, and C_2 are the amplitudes corresponding to the ${}^3P_0 \to {}^1S_0s$, ${}^3S_1 \to {}^1S_0p$, and ${}^3D_1 \to {}^1S_0p$ transitions, in order. They are related to the corresponding amplitudes in the JLS basis via

$$A_1 = \frac{1}{\sqrt{3}}\,\mathcal{A}^{\rm full}\big[{}^3P_0,\, {}^1S_0\big], \tag{A9}$$

$$C_1 = \mathcal{A}^{\rm full}\big[{}^3S_1,\, {}^1S_0\big], \tag{A10}$$

$$C_2 = \frac{3}{\sqrt{2}}\,\mathcal{A}^{\rm full}\big[{}^3D_1,\, {}^1S_0\big]. \tag{A11}$$

The observables we consider are expressed in terms of these amplitudes in the following way:

$$\begin{aligned}\frac{d^2\sigma}{d\Omega dm_{pp}^2} = {}& \frac{1}{4\Delta M_{pp}^2}\frac{1}{(4\pi)^4 M_N sp}\int_0^{p_{\rm cut}} k_\pi(p')p'^2dp' \\ & \times\Bigg\{|A_1|^2 + \left|C_1 - \frac{C_2}{3}\right|^2 \\ & + 2{\rm Re}\left[A_1^*\left(C_1 + \frac{2C_2}{3}\right)\right]\cos\theta_\pi \\ & + \left[2{\rm Re}\,(C_2^*C_1) + \frac{|C_2|^2}{3}\right]\cos^2\theta_\pi\Bigg\},\end{aligned} \tag{A12}$$

$$A_y \times \frac{d^2\sigma}{d\Omega dm_{pp}^2} = \frac{1}{4\Delta M_{pp}^2}\frac{1}{(4\pi)^4 M_N s p}\int_0^{p_{\rm cut}} k_\pi(p') p'^2 dp' \times \left\{ \sin 2\theta_\pi \, {\rm Im}\,(C_1^* C_2) - 2\sin\theta_\pi \, {\rm Im}\left[A_1^* \left(C_1 - \frac{C_2}{3}\right)\right]\right\}, \quad \text{(A13)}$$

where $p_{\rm cut}$ is the maximum relative momentum of the final protons in the measurements at TRIUMF [44,45], $\Delta M_{pp}^2 = (2M_N + p_{\rm cut}^2/M_N)^2 - (2M_N)^2 \approx 4p_{\rm cut}^2$, $k_\pi(p')$ is the momentum of the final pion, and s and p are the invariant energy squared and the relative momentum of the initial nucleons, in order.

Below we give the expressions for the tree amplitudes $\mathcal{A}[^3S_1, {}^1S_0], \mathcal{A}[^3D_1, {}^1S_0]$ resulting from various pion production mechanisms as well as those for the relevant production amplitudes involving the Δ isobar. Note that from here on we suppress the label "tree" on the tree-level transition amplitudes. We also explain how we extract A_1 from experimental data.

a. Direct production

$$\mathcal{A}[^3S_1, {}^1S_0](p, p') = C\int \frac{d\Omega_{\vec{k}_\pi}}{4\pi}\left[-k_\pi + \frac{\omega_\pi}{M_N}(\vec{p}\,'\hat{k}_\pi)\right] \times (2\pi)^3\delta^{(3)}(\vec{p}\,' - \vec{p} + \vec{k}_\pi/2), \quad \text{(A14)}$$

$$\mathcal{A}[^3D_1, {}^1S_0](p, p') = \frac{C}{\sqrt{2}}\int \frac{d\Omega_{\vec{k}_\pi}}{4\pi}\left[-k_\pi[3(\hat{p}\hat{k}_\pi)^2 - 1] + \frac{\omega_\pi}{M_N}[3(\hat{p}\hat{k}_\pi)(\hat{p}\,\vec{p}\,') - (\vec{p}\,'\hat{k}_\pi)]\right] \times (2\pi)^3\delta^{(3)}(\vec{p}\,' - \vec{p} + \vec{k}_\pi/2), \quad \text{(A15)}$$

where $C = -{\rm i}\frac{8M_N^2 g_A}{f_\pi\sqrt{2}}$ and $\omega_\pi = \sqrt{k_\pi^2 + m_\pi^2}$ is the energy of the final pion. Here we included both the leading πNN vertex and its recoil correction that enters at NNLO.

b. Production via the $\Delta(1232)$ *isobar*

The $\Delta(1232)$ contribution comes from the $N\Delta$ intermediate states. In the reaction $pn \to pp\pi^-$ with the initial isospin of the pn system being $I = 0$, the $N\Delta \leftrightarrow NN$ transitions are allowed only in the final-state interaction. As we consider those kinematical configurations where the relative kinetic energy of the final protons is small, it is only the $^1S_0$ final state that contributes. Therefore, the only coupled channels where the $\Delta(1232)$ contributes is $^5D_0(N\Delta) \to {}^1S_0(NN)$. For p-wave pions the relevant amplitudes that correspond to the $^3S_1(NN) \to {}^5D_0(N\Delta)$ and $^3D_1(NN) \to {}^5D_0(N\Delta)$ transitions in the production operator read:

$$\mathcal{A}\big[^3S_1, {}^5D_0\big](p, p') = C_\Delta\int \frac{d\Omega_{\vec{k}_\pi}}{4\pi}\{-k_\pi[3(\hat{p}\,'\hat{k}_\pi)^2 - 1]\} \times (2\pi)^3\delta^{(3)}(\vec{p}\,' - \vec{p} + \vec{k}_\pi\vartheta), \quad \text{(A16)}$$

$$\mathcal{A}\big[^3D_1, {}^5D_0\big](p, p') = \frac{C_\Delta}{\sqrt{2}}\int \frac{d\Omega_{\vec{k}_\pi}}{4\pi}\{-k_\pi[9(\hat{p}\,'\hat{p})(\hat{p}\,'\hat{k}_\pi)(\hat{p}\hat{k}_\pi) - 3(\hat{p}\hat{k}_\pi)^2 - 3(\hat{p}\,'\hat{k}_\pi)^2 + 1]\} \times (2\pi)^3\delta^{(3)}(\vec{p}\,' - \vec{p} + \vec{k}_\pi\vartheta), \quad \text{(A17)}$$

where $C_\Delta = -{\rm i}\frac{8M_N M_\Delta h_A}{3f_\pi\sqrt{2}}\sqrt{\frac{M_N}{M_\Delta}}$, and $\vartheta = \frac{M_N}{M_N + M_\Delta}$ and p' is the relative momentum of the $N\Delta$ state.

c. Rescattering via the s-wave WT vertex

$$\mathcal{A}[^3S_1, {}^1S_0](p, p') = -\frac{C\,\omega_\pi k_\pi}{2f_\pi^2}\int \frac{d\Omega_{\vec{p}}}{4\pi}\frac{1}{(\vec{p} - \vec{p}\,')^2 + m_\pi^2} \times \left[1 - \frac{2(\vec{p} - \vec{p}\,')^2}{3\big[(\vec{p} - \vec{p}\,')^2 + m_\pi^2\big]}\right], \quad \text{(A18)}$$

$$\mathcal{A}[^3D_1, {}^1S_0](p, p') = \frac{C\,\omega_\pi k_\pi}{3f_\pi^2\sqrt{2}}\int \frac{d\Omega_{\vec{p}}}{4\pi} \times \frac{3(\vec{p}\,'\hat{p} - p)^2 - (\vec{p} - \vec{p}\,')^2}{\big[(\vec{p} - \vec{p}\,')^2 + m_\pi^2\big]^2}. \quad \text{(A19)}$$

Note that in these expressions, and also in the expressions for the amplitudes that stem from operators with c_3, c_4, and recoil corrections to the WT vertex (see below), we keep only the leading term in the expansion in powers of k_π/p. The same is true for the corresponding amplitudes in the reactions $pp \to d\pi^+$ and $pp \to pn\pi^+$.

d. Operators with c_3, c_4, *and recoil corrections to the WT vertex*

$$\mathcal{A}[^3S_1, {}^1S_0](p, p') = \frac{4C\,k_\pi}{3f_\pi^2}\int \frac{d\Omega_{\vec{p}\,'}}{4\pi}\left[C_i^{^3S_1}\frac{(\vec{p} - \vec{p}\,')^2}{(\vec{p} - \vec{p}\,')^2 + m_\pi^2} + \frac{1}{8M_N}\frac{p'^2 - p^2}{(\vec{p} - \vec{p}\,')^2 + m_\pi^2}\right], \quad \text{(A20)}$$

$$\mathcal{A}[^3D_1, {}^1S_0](p, p') = \frac{2C\,k_\pi}{3f_\pi^2\sqrt{2}}\int \frac{d\Omega_{\vec{p}\,'}}{4\pi} \times \left\{C_i^{^3D_1}\frac{3(\vec{p}\,'\hat{p} - p)^2 - (\vec{p} - \vec{p}\,')^2}{(\vec{p} - \vec{p}\,')^2 + m_\pi^2} + \frac{1}{4M_N}\frac{3[(\vec{p}\,'\hat{p})^2 - p^2] - p'^2 + p^2}{(\vec{p} - \vec{p}\,')^2 + m_\pi^2}\right\}, \quad \text{(A21)}$$

where $C_i^{^3S_1} = \frac{c_3}{2} + c_4 + \frac{1}{4M_N}$, $C_i^{^3D_1} = c_3 - c_4 - \frac{1}{4M_N}$.

e. Contact term

$$\mathcal{A}\big[^3S_1, {}^1S_0\big](p, p') = \frac{2C\,k_\pi}{g_A}d, \quad \text{(A22)}$$

$$\mathcal{A}\big[^3D_1, {}^1S_0\big](p, p') = 0. \quad \text{(A23)}$$

f. Coulomb interaction

Because the final two protons are at low relative momenta, there are sizable effects from the Coulomb interaction between the two protons. The effect of the Coulomb interaction was taken into account along the lines of Refs. [67,68]. To be specific, we multiply all tree diagrams that do not contain the Δ isobar by the Gamow-Sommerfeld factor

$$G(p') = \left[\frac{2\pi\gamma(p')}{\exp 2\pi\gamma(p') - 1}\right]^{1/2}, \qquad \gamma(p') = \frac{M_N}{2\alpha p'}, \tag{A24}$$

where α is the electromagnetic fine structure constant. At the same time, the half–off-shell $pp\,\mathcal{M}$ matrix in the ${}^1S_0$ partial wave that we use in our calculation is corrected for the Coulomb interaction according to

$$\mathcal{M}^{\rm CC}(q, p') = \mathcal{M}(q, p')\frac{G(q)}{G(p')}\frac{\mathcal{M}^{\rm CC}(p', p')}{\mathcal{M}(p', p')}, \tag{A25}$$

where $\mathcal{M}(q, p')$ and $\mathcal{M}^{\rm CC}(q, p')$ are, in order, the half–off-shell $pp\,\mathcal{M}$ matrices without and with the inclusion of the Coulomb interaction, whereas $\mathcal{M}(p', p')$ and $\mathcal{M}^{\rm CC}(p', p')$ are the corresponding pp on-shell $\mathcal{M}$ matrices. See Ref. [67] for more details.

As far as diagrams with the Δ are concerned, where we have the transition ${}^5D_0(N\Delta) \to {}^1S_0(NN)$, we apply the following argument to take into account the Coulomb interaction. First, we note that the typical relative momenta of the intermediate $N\Delta$ state are large so that the Coulomb interaction in this intermediate state is expected to be unimportant. To take into account the Coulomb interaction between the protons in the final state, we multiply the amplitude with $N\Delta$ by the ratio of the inverse Jost functions

$$G_{N\Delta}(p') = \frac{F^{\rm CC}_{pp}(p')}{F_{pp}(p')}, \tag{A26}$$

where $F^{\rm CC}_{pp}(p')$ and $F_{pp}(p')$ are the pp inverse Jost functions with and without Coulomb interaction, respectively. They are related to the corresponding $\mathcal{M}$ matrices via

$$F^{\rm CC}_{pp}(p') = G(p') + \frac{1}{4M_N}\int\frac{d^3q}{(2\pi)^3}\frac{G(q)\mathcal{M}^{\rm CC}(q, p')}{q^2 - p'^2 - i0}, \tag{A27}$$

$$F_{pp}(p') = 1 + \frac{1}{4M_N}\int\frac{d^3q}{(2\pi)^3}\frac{\mathcal{M}(q, p')}{q^2 - p'^2 - i0}. \tag{A28}$$

Notice that the overall normalization of the Jost functions is of no relevance, for they occur only in the ratio (however, both Jost functions have to have the same normalization factors).

g. The contribution of the $I = 1$ initial state

We write A_1 in Eq. (A8) in a form that takes into account the ISI phase as well as the dependence of the final-state Jost function on the momenta:

$$A_1 = {\rm i}\,X\exp({\rm i}\delta^{^3P_0})F^{\rm CC}_{pp}(p'). \tag{A29}$$

The constant (real) factor X is adjusted in such a way to reproduce the corresponding amplitude extracted from the TRIUMF data using a partial-wave analysis [45,47]. The sign of X is adjusted to the behavior of observables in $pn \to pp\pi^-$.

3. The reaction $pp \to d\pi^+$

The transitions that contribute to the reaction $pp \to d\pi^+$ at energies close to threshold are ${}^1S_0 \to {}^3S_1 p$, ${}^1S_0 \to {}^3D_1 p$, ${}^1D_2 \to {}^3S_1 p$, ${}^1D_2 \to {}^3D_1 p$, and ${}^3P_1 \to {}^3S_1 s$, ${}^3P_1 \to {}^3D_1 s$. The spin-angular structure of the amplitude reads

$$\mathcal{M}_{pp\to d\pi^+} = \{C_0(\vec{\mathcal{S}}\times\hat{p})\vec{\varepsilon} + C_1\mathcal{I}(\hat{k}\vec{\varepsilon}) + C_2\mathcal{I}[(\hat{p}\hat{k})(\hat{p}\vec{\varepsilon}) - \tfrac{1}{3}(\hat{k}\vec{\varepsilon})]\}, \tag{A30}$$

where $\vec{\varepsilon}$ is the deuteron polarization vector, $\vec{\mathcal{S}} = \chi_2^T\frac{\sigma_2}{\sqrt{2}}\vec{\sigma}\chi_1$, $\mathcal{I} = \chi_2^T\frac{\sigma_2}{\sqrt{2}}\chi_1$ are normalized spin structures corresponding to the initial spin-triplet and spin-singlet states, in order. Here, the χ's refer to spinors of the initial nucleons, and C_0, C_1, and C_2 are the amplitudes corresponding to the ${}^3P_1 \to \vec{\varepsilon}\,s$, ${}^1S_0 \to \vec{\varepsilon}\,p$, and ${}^1D_2 \to \vec{\varepsilon}\,p$ transitions, in order. Further, we denote the final states as $\vec{\varepsilon}\,l$, where $\vec{\varepsilon}$ stands for the deuteron final state, and l is the angular momentum of the final pion relative to the deuteron. The amplitudes C_0, C_1, and C_2 are related to the corresponding amplitudes in JLS basis via

$$C_0 = \sqrt{\frac{3}{2}}\,\mathcal{A}^{\rm full}[{}^3P_1, 1], \tag{A31}$$

$$C_1 = \mathcal{A}^{\rm full}[{}^1S_0, 1], \tag{A32}$$

$$C_2 = \sqrt{\frac{15}{2}}\,\mathcal{A}^{\rm full}[{}^1D_2, 1]. \tag{A33}$$

Note that, as it can be seen from Eq. (A6), the amplitudes of the transitions to the deuteron state are sums of the amplitudes where the transition goes to the S-wave component and those where the transition goes to the D-wave component of the deuteron wave function. Note also that here the total amplitudes are distinguished only by the initial state, as the final state, the deuteron, is the same for all transitions. However, at the level of tree amplitudes, one has to distinguish between the ones that correspond to transitions to the S-wave component and those to the D-wave component.

The observables under consideration are expressed through the amplitudes C_0, C_1, and C_2 as

$$\frac{d\sigma}{d\Omega} = \frac{k_\pi}{256\pi^2 sp}\left[2|C_0|^2 + |C_1|^2 + \frac{1}{9}|C_2|^2(3\cos^2\theta_\pi + 1) + \frac{2}{3}{\rm Re}\,(C_1C_2^*)(3\cos^2\theta_\pi - 1)\right], \tag{A34}$$

$$A_y \times \frac{d\sigma}{d\Omega} = \frac{k_\pi}{256\pi^2 sp} \times 2\sin\theta_\pi \cos\phi \ \mathrm{Im}\left[C_0^*\left(C_1 - \frac{C_2}{3}\right)\right]. \quad \text{(A35)}$$

Below, we give expressions for the tree amplitudes $\mathcal{A}[^1D_2, {}^3D_1]$, $\mathcal{A}[^1D_2, {}^3S_1]$, $\mathcal{A}[^1S_0, {}^3D_1]$, $\mathcal{A}[^1S_0, {}^3S_1]$, contributing to C_1 and C_2, as well as those for the relevant production amplitudes involving the Δ isobar. We also provide details of the determination of C_0.

a. Direct production

$$\mathcal{A}\big[^1S_0, {}^3S_1\big](p, p') = C\int \frac{d\Omega_{\vec{k}_\pi}}{4\pi}\left[-k_\pi + \frac{\omega_\pi}{M_N}(\vec{p}\,'\hat{k}_\pi)\right] \times (2\pi)^3\delta^{(3)}(\vec{p}\,' - \vec{p} + \vec{k}_\pi/2), \quad \text{(A36)}$$

$$\mathcal{A}\big[^1S_0, {}^3D_1\big](p, p') = \frac{C}{\sqrt{2}}\int \frac{d\Omega_{\vec{k}_\pi}}{4\pi}\left\{-k_\pi[3(\hat{p}\,'\hat{k}_\pi)^2 - 1] + \frac{2\omega_\pi}{M_N}(\vec{p}\,'\hat{k}_\pi)\right\}(2\pi)^3\delta^{(3)}(\vec{p}\,' - \vec{p} + \vec{k}_\pi/2), \quad \text{(A37)}$$

$$\mathcal{A}\big[^1D_2, {}^3S_1\big](p, p') = C\sqrt{\frac{3}{10}}\int \frac{d\Omega_{\vec{k}_\pi}}{4\pi}\left\{-k_\pi[3(\hat{p}\hat{k}_\pi)^2 - 1] + \frac{\omega_\pi}{M_N}[3(\hat{p}\,\vec{p}\,')(\hat{p}\hat{k}_\pi) - \vec{p}\,'\hat{k}_\pi]\right\} \times (2\pi)^3\delta^{(3)}(\vec{p}\,' - \vec{p} + \vec{k}_\pi/2), \quad \text{(A38)}$$

$$\mathcal{A}\big[^1D_2, {}^3D_1\big](p, p') = \frac{C}{\sqrt{2}}\sqrt{\frac{3}{10}}\int \frac{d\Omega_{\vec{k}_\pi}}{4\pi}\left\{-k_\pi[9(\hat{p}\,'\hat{k}_\pi) \times (\hat{p}\,'\hat{p})(\hat{p}\hat{k}_\pi) - 3(\hat{p}\hat{k}_\pi)^2 - 3(\hat{p}\,'\hat{k}_\pi)^2 + 1] + \frac{2\omega_\pi}{M_N}[3(\hat{p}\,\vec{p}\,')(\hat{p}\hat{k}_\pi) - \vec{p}\,'\hat{k}_\pi]\right\} \times (2\pi)^3\delta^{(3)}(\vec{p}\,' - \vec{p} + \vec{k}_\pi/2). \quad \text{(A39)}$$

b. Production via the $\Delta(1232)$ *isobar*

In the reaction $pp \to d\pi^+$, the initial isospin of the pp system is $I = 1$, so the $N\Delta \leftrightarrow NN$ intermediate states are allowed only in the initial-state interaction. The coupled channels that contribute are[3] $^1S_0(NN) \to {}^5D_0(N\Delta)$, $^1D_2(NN) \to {}^5D_2(N\Delta)$, and $^1D_2(NN) \to {}^5S_2(N\Delta)$. The relevant transitions in the production operator for p-wave pions are $^5D_0(N\Delta) \to {}^3S_1(NN)$, $^5D_0(N\Delta) \to {}^3D_1(NN)$, $^5D_2(N\Delta) \to {}^3S_1(NN)$, $^5D_2(N\Delta) \to {}^3D_1(NN)$, $^5S_2(N\Delta) \to {}^3S_1(NN)$, and $^5S_2(N\Delta) \to {}^3D_1(NN)$. The expressions for the correspondingxs amplitudes read:

$$\mathcal{A}\big[^5D_0, {}^3S_1\big](p, p') = C_\Delta\int \frac{d\Omega_{\vec{k}_\pi}}{4\pi}\{-k_\pi[3(\hat{p}\hat{k}_\pi)^2 - 1]\} \times (2\pi)^3\delta^{(3)}(\vec{p}\,' - \vec{p} + \vec{k}_\pi/2), \quad \text{(A40)}$$

$$\mathcal{A}\big[^5D_0, {}^3D_1\big](p, p') = \frac{C_\Delta}{\sqrt{2}}\int\frac{d\Omega_{\vec{k}_\pi}}{4\pi}\{-k_\pi[9(\hat{p}\,'\hat{p})(\hat{p}\,'\hat{k}_\pi)(\hat{p}\hat{k}_\pi) - 3(\hat{p}\hat{k}_\pi)^2 - 3(\hat{p}\,'\hat{k}_\pi)^2 + 1]] \times (2\pi)^3\delta^{(3)}(\vec{p}\,' - \vec{p} + \vec{k}_\pi/2), \quad \text{(A41)}$$

$$\mathcal{A}\big[^5D_2, {}^3S_1\big](p, p') = C_\Delta\sqrt{\frac{21}{20}}\int \frac{d\Omega_{\vec{k}_\pi}}{4\pi}\big[-k_\pi[3(\hat{p}\hat{k}_\pi)^2 - 1]\big] \times (2\pi)^3\delta^{(3)}(\vec{p}\,' - \vec{p} + \vec{k}_\pi/2), \quad \text{(A42)}$$

$$\mathcal{A}\big[^5D_2, {}^3D_1\big](p, p') = \frac{3}{4}C_\Delta\sqrt{\frac{6}{35}}\int \frac{d\Omega_{\vec{k}_\pi}}{4\pi}\left[-k_\pi\left[9(\hat{p}\,\hat{p}\,')^2 - 6(\hat{p}\,\hat{p}\,')(\hat{p}\hat{k}_\pi)(\hat{p}\,'\hat{k}_\pi) + 2(\hat{p}\hat{k}_\pi)^2 + 2(\hat{p}\,'\hat{k}_\pi)^2 - \frac{11}{3}\right]\right] \times (2\pi)^3\delta^{(3)}(\vec{p}\,' - \vec{p} + \vec{k}_\pi/2), \quad \text{(A43)}$$

$$\mathcal{A}\big[^5S_2, {}^3S_1\big](p, p') = C_\Delta\sqrt{6}\int \frac{d\Omega_{\vec{k}_\pi}}{4\pi}[-k_\pi] \times (2\pi)^3\delta^{(3)}(\vec{p}\,' - \vec{p} + \vec{k}_\pi/2), \quad \text{(A44)}$$

$$\mathcal{A}\big[^5S_2, {}^3D_1\big](p, p') = \frac{\sqrt{3}}{10}C_\Delta\int \frac{d\Omega_{\vec{k}_\pi}}{4\pi}\big[-k_\pi[3(\hat{p}\,'\hat{k}_\pi)^2 - 1]\big] \times (2\pi)^3\delta^{(3)}(\vec{p}\,' - \vec{p} + \vec{k}_\pi/2). \quad \text{(A45)}$$

c. Rescattering via the s-wave WT vertex

$$\mathcal{A}\big[^1S_0, {}^3S_1\big](p, p') = \frac{C\,\omega_\pi k_\pi}{2f_\pi^2}\int\frac{d\Omega_{\vec{p}}}{4\pi}\frac{1}{(\vec{p} - \vec{p}\,')^2 + m_\pi^2} \times \left[1 - \frac{2(\vec{p} - \vec{p}\,')^2}{3\big[(\vec{p} - \vec{p}\,')^2 + m_\pi^2\big]}\right], \quad \text{(A46)}$$

$$\mathcal{A}\big[^1S_0, {}^3D_1\big](p, p') = -\frac{C\,\omega_\pi k_\pi}{3f_\pi^2\sqrt{2}}\int\frac{d\Omega_{\vec{p}}}{4\pi} \times \frac{3(\vec{p}\hat{p}' - p')^2 - (\vec{p} - \vec{p}\,')^2}{\big[(\vec{p} - \vec{p}\,')^2 + m_\pi^2\big]^2}, \quad \text{(A47)}$$

$$\mathcal{A}\big[^1D_2, {}^3S_1\big](p, p') = -\frac{C\,\omega_\pi k_\pi}{f_\pi^2\sqrt{30}}\int\frac{d\Omega_{\vec{p}'}}{4\pi} \times \frac{3(\vec{p}\,'\hat{p} - p)^2 - (\vec{p} - \vec{p}\,')^2}{\big[(\vec{p} - \vec{p}\,')^2 + m_\pi^2\big]^2}, \quad \text{(A48)}$$

[3]We do not take into account the channel $^1D_2(NN) \to {}^3D_2(N\Delta)$ because the corresponding $NN \to N\Delta\,\mathcal{M}$ matrix is subleading according to the power counting and it is also numerically small at the energies considered [37].

$$\mathcal{A}[{}^1D_2, {}^3D_1](p, p') = \frac{3}{\sqrt{2}} \frac{C\,\omega_\pi k_\pi}{f_\pi^2\sqrt{30}} \int \frac{d\Omega_{\vec{p}'}}{4\pi} \frac{1}{(\vec{p}-\vec{p}\,')^2+m_\pi^2} \left[\frac{3(\hat{p}\hat{p}')^2-1}{2} - \frac{9(p-\vec{p}\,'\hat{p})(\vec{p}\hat{p}'-p')(\hat{p}\hat{p}') - 3(p-\vec{p}\,'\hat{p})^2 - 3(p'-\vec{p}\hat{p}')^2 + (\vec{p}-\vec{p}\,')^2}{3[(\vec{p}-\vec{p}\,')^2+m_\pi^2]} \right]. \tag{A49}$$

d. Operators with c_3, c_4, and recoil corrections to the WT vertex

$$\mathcal{A}[{}^1S_0, {}^3S_1](p, p') = \frac{4C\,k_\pi}{3f_\pi^2} \int \frac{d\Omega_{\vec{p}'}}{4\pi} \left[C_i^{{}^3S_1} \frac{(\vec{p}-\vec{p}\,')^2}{(\vec{p}-\vec{p}\,')^2+m_\pi^2} + \frac{1}{8M_N} \frac{p^2-p'^2}{(\vec{p}-\vec{p}\,')^2+m_\pi^2} \right], \tag{A50}$$

$$\mathcal{A}[{}^1S_0, {}^3D_1](p, p') = \frac{2C\,k_\pi}{3f_\pi^2\sqrt{2}} \int \frac{d\Omega_{\vec{p}'}}{4\pi} \left\{ C_i^{{}^3D_1} \frac{3(\vec{p}\hat{p}'-p')^2-(\vec{p}-\vec{p}\,')^2}{(\vec{p}-\vec{p}\,')^2+m_\pi^2} + \frac{1}{4M_N} \frac{3[(\vec{p}\hat{p}')^2-p'^2]-p^2+p'^2}{(\vec{p}-\vec{p}\,')^2+m_\pi^2} \right\}, \tag{A51}$$

$$\mathcal{A}[{}^1D_2, {}^3S_1](p, p') = \frac{2C\,k_\pi}{f_\pi^2\sqrt{30}} \int \frac{d\Omega_{\vec{p}'}}{4\pi} \left\{ C_i^{{}^3D_1} \frac{3(\vec{p}\,'\hat{p}-p)^2-(\vec{p}-\vec{p}\,')^2}{(\vec{p}-\vec{p}\,')^2+m_\pi^2} - \frac{1}{4M_N} \frac{3[(\vec{p}\,'\hat{p})^2-p^2]-p'^2+p^2}{(\vec{p}-\vec{p}\,')^2+m_\pi^2} \right\}, \tag{A52}$$

$$\begin{aligned}\mathcal{A}[{}^1D_2, {}^3D_1](p, p') = \frac{C\,k_\pi}{f_\pi^2\sqrt{15}} \int \frac{d\Omega_{\vec{p}'}}{4\pi} \Bigg[& C_i^{{}^3D_1} \left\{ \frac{9(p-\vec{p}\,'\hat{p})(\vec{p}\hat{p}'-p')(\hat{p}\hat{p}')}{(\vec{p}-\vec{p}\,')^2+m_\pi^2} + \frac{-3(p-\vec{p}\,'\hat{p})^2-3(p'-\vec{p}\hat{p}')^2+(\vec{p}-\vec{p}\,')^2}{(\vec{p}-\vec{p}\,')^2+m_\pi^2} \right\} \\ & - \frac{1}{4M_N} \left\{ \frac{9(\vec{p}\,'\hat{p}+p)(p'-\vec{p}\hat{p}')(\hat{p}\hat{p}')}{(\vec{p}-\vec{p}\,')^2+m_\pi^2} + \frac{-3(p'+\vec{p}\hat{p}')(p'-\vec{p}\hat{p}')-3(\vec{p}\,'\hat{p}+p)(\vec{p}\,'\hat{p}-p)+p'^2-p^2}{(\vec{p}-\vec{p}\,')^2+m_\pi^2} \right\} \\ & + 3\left(c_4+\frac{1}{4M_N}\right) \frac{[3(\hat{p}\hat{p}')^2-1](\vec{p}-\vec{p}\,')^2}{(\vec{p}-\vec{p}\,')^2+m_\pi^2} \Bigg]. \end{aligned} \tag{A53}$$

e. Contact term

$$\mathcal{A}[{}^1S_0, {}^3S_1](p, p') = \frac{2C\,k_\pi}{g_A} d, \tag{A54}$$

$$\mathcal{A}[{}^1S_0, {}^3D_1](p, p') = 0, \tag{A55}$$

$$\mathcal{A}[{}^1D_2, {}^3S_1](p, p') = 0, \tag{A56}$$

$$\mathcal{A}[{}^1D_2, {}^3D_1](p, p') = 0. \tag{A57}$$

f. Coulomb interaction

For this reaction, the Coulomb interaction between the initial protons gives only a small effect because the initial relative momentum is large. On the contrary, the deuteron and pion in the final state are at low relative momenta, and the Coulomb interaction between them is taken into account at the level of experimental data by factoring out the Gamow-Sommerfeld factors that stem from the $\pi^+ d$ Coulomb interaction; see, e.g., Ref. [54].

g. Pion production in the s wave

To calculate the amplitude of the s-wave pion production, that is, the value of C_0, we took the result of Refs. [17,69], where the amplitude of the s-wave pion production was calculated up to NLO. We correct this amplitude by a constant factor to get at threshold the value of s-wave production parameter $\alpha = 252\ \mu$b. This quantity, α, is the total cross section divided by the final pion momentum in units of the pion mass, and the given value is extracted from the width of pionic deuterium [50,51].

4. The reaction $pp \to pn\pi^+$

The transitions that contribute to the reaction $pp \to pn\pi^+$ at energies close to threshold are ${}^1S_0 \to {}^3S_1 p$, ${}^1S_0 \to {}^3D_1 p$, ${}^1D_2 \to {}^3S_1 p$, ${}^1D_2 \to {}^3D_1 p$, and ${}^3P_1 \to {}^3S_1 s$, ${}^3P_1 \to {}^3D_1 s$. At very low energies, the final ${}^3D_1$ state does not contribute, however, the transitions to the ${}^3D_1$ state contribute via the ${}^3D_1 \leftrightarrow {}^3S_1$ coupled channels. At these low energies, the spin-angular structure of the amplitude reads

$$\begin{aligned}\mathcal{M}_{pp\to pn\pi^+} = & \left[\tilde{C}_0 (\vec{\mathcal{S}} \times \hat{p}\,) \vec{\mathcal{S}}\,' + \tilde{C}_1 \mathcal{I}(\hat{k}\vec{\mathcal{S}}\,') \right. \\ & \left. + \tilde{C}_2\, \mathcal{I}[(\hat{p}\hat{k})(\hat{p}\vec{\mathcal{S}}\,') - \tfrac{1}{3}(\hat{k}\vec{\mathcal{S}}\,')]\right], \end{aligned} \tag{A58}$$

where $\vec{\mathcal{S}} = \chi_2^T \frac{\sigma_2}{\sqrt{2}} \vec{\sigma}\, \chi_1$, $\mathcal{I} = \chi_2^T \frac{\sigma_2}{\sqrt{2}} \chi_1$, $\vec{\mathcal{S}}\,' = \chi_{1'}^\dagger \vec{\sigma} \frac{\sigma_2}{\sqrt{2}} \chi_{2'}^*$ are normalized spin structures corresponding to the initial spin-triplet, initial spin-singlet, and final spin-triplet states, in order. Here, $\tilde{C}_0$, $\tilde{C}_1$, and $\tilde{C}_2$ are the amplitudes corresponding to the ${}^3P_1 \to {}^3S_1 s$, ${}^1S_0 \to {}^3S_1 p$, and ${}^1D_2 \to {}^3S_1 p$ transitions, in order. Their relation with the corresponding amplitudes in the JLS

basis is given by

$$\tilde{C}_0 = \sqrt{\frac{3}{2}}\,\mathcal{A}^{\rm full}\big[{}^3P_1, {}^3S_1\big], \tag{A59}$$

$$\tilde{C}_1 = \mathcal{A}^{\rm full}\big[{}^1S_0, {}^3S_1\big], \tag{A60}$$

$$\tilde{C}_2 = \sqrt{\frac{15}{2}}\,\mathcal{A}^{\rm full}\big[{}^1D_2, {}^3S_1\big]. \tag{A61}$$

In addition to these amplitudes, there are also amplitudes that correspond to the transition to the isospin-1 ${}^1S_0$ final pn state. However, these amplitudes do not interfere with $\tilde{C}_0$, $\tilde{C}_1$, and $\tilde{C}_2$ because of different spins in the final state and generate only an additive part in the cross section—see also the discussion in the text. The observables in the reaction $pp \to pn\pi^+$ can be expressed through $\tilde{C}_0$, $\tilde{C}_1$, and $\tilde{C}_2$ in the following way:

$$\frac{d\sigma}{d\Omega} = \frac{1}{2(4\pi)^4 M_N s p}\int_0^{p_{\rm max}} k_\pi(p') p'^2 dp' \times \left[2|\tilde{C}_0|^2 + |\tilde{C}_1|^2 + \frac{1}{9}|\tilde{C}_2|^2(3\cos^2\theta_\pi + 1) + \frac{2}{3}{\rm Re}\,(\tilde{C}_1\tilde{C}_2^*)(3\cos^2\theta_\pi - 1)\right] + \frac{d\sigma}{d\Omega}^{I=1} \tag{A62}$$

$$A_y \times \frac{d\sigma}{d\Omega} = \frac{1}{2(4\pi)^4 M_N s p}\int_0^{p_{\rm max}} k_\pi(p') p'^2 dp' \times 2\sin\theta_\pi\cos\phi\ {\rm Im}\left[\tilde{C}_0^*\left(\tilde{C}_1 - \frac{\tilde{C}_2}{3}\right)\right]. \tag{A63}$$

Here, $p_{\rm max}$ is the maximum relative momentum of the final nucleons, and $\frac{d\sigma}{d\Omega}^{I=1}$ is the contribution of the final pn state with isospin 1 to the cross section.

The expressions for the transition matrix elements relevant for the calculation of $\tilde{C}_1$ and $\tilde{C}_2$ are the same as for the reaction $pp \to d\pi^+$, and therefore we refer the reader to the corresponding formulas, given in Sec. A3 above. However, we should make a remark about the value of $\tilde{C}_0$. Instead of calculating it at NLO we extracted $\tilde{C}_0$ directly from the data—see the discussion in the main text.

APPENDIX B: RESONANCE SATURATION VS. EXPLICIT DELTA

In the chiral limit the masses of both the Δ and the nucleon stay finite and differ from each other. Thus, there is a well-defined limit of QCD where $m_\pi/\Delta M$, with $\Delta M = M_\Delta - M_N$, is a small parameter. Consequently, the Δ degrees of freedom may be integrated out and the effects of the Δ isobar are then absorbed into the LECs of the resulting Lagrangian. However, when the Δ degrees of freedom are included dynamically in the NN system, certain selection rules apply. In particular, the Δ is allowed to contribute only if the NN system has the total isospin equal to 1. It is instructive to discuss the implications of these selection rules for the reaction $NN \to NN\pi$ using both the EFT with and without explicit Δ degrees of freedom. The corresponding discussion for πN scattering can be found in Ref. [41].

For simplicity, let us start from elastic πN scattering. Using the interactions defined in the main text one finds straightforwardly for diagram (a) of Fig. 9 in the limit $\Delta M \to \infty$

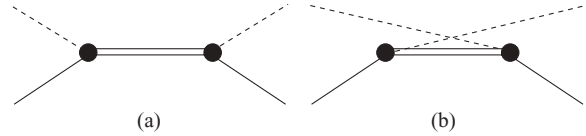

FIG. 9. Leading diagrams for πN scattering with intermediate Δ. Shown are the s-channel (a) and the u-channel (b) contribution.

$$iA^{\pi\ {\rm elast}}_{(a)} = -i\left(\frac{2M_N h_A^2}{4f_\pi^2\Delta M}\right)(\vec{S}\cdot\vec{q}\,')T_b(\vec{S}^\dagger\cdot\vec{q})T_a^\dagger = -i\left(\frac{M_N h_A^2}{18 f_\pi^2\Delta M}\right)q'_i q_j(2\delta_{ij} - i\epsilon_{ijk}\sigma_k) \times (2\delta_{ba} - i\epsilon_{bac}\tau_c), \tag{B1}$$

where a (b) and $\vec{q}$ ($\vec{q}\,'$) denote the isospin quantum number and momentum of the incoming (outgoing) pion. Analogously, one finds for the u-channel diagram

$$iA^{\pi\ {\rm elast}}_{(b)} = -i\left(\frac{2M_N h_A^2}{4f_\pi^2\Delta M}\right)(\vec{S}\cdot\vec{q})T_a(\vec{S}^\dagger\cdot\vec{q}\,')T_b^\dagger = -i\left(\frac{M_N h_A^2}{18 f_\pi^2\Delta M}\right)q'_i q_j(2\delta_{ij} - i\epsilon_{jik}\sigma_k) \times (2\delta_{ba} - i\epsilon_{abc}\tau_c). \tag{B2}$$

In the second line of the above equation we used Eqs. (4). Thus, Figs. 9(a) and 9(b) are individually given by four terms. However, two of them get canceled when adding the contributions together. The remaining two terms in the sum exactly resemble the structure of the c_3 and c_4 terms of the effective Lagrangian. One then finds for the Δ contribution to the LECs c_i the following result [41]:

$$c_3^\Delta = -2c_4^\Delta = \frac{h_A^2}{9\Delta M}. \tag{B3}$$

Obviously this matching is only possible after adding the two diagrams together. However, the above-mentioned selection rules for $NN \to NN\pi$ are operative at the level of the individual diagrams. We now show how these two facts can be realized simultaneously.

In full analogy to the expressions given above, one finds for the amplitudes corresponding to the diagrams of Fig. 2 involving the Δ:

$$iA_{(c)} = -\left(\frac{M_N^2 g_A h_A^2}{18 f_\pi^3\Delta M}\right)\tau_a^{(2)}(\sigma^{(2)}\cdot\vec{q})\frac{1}{q^2 - m_\pi^2}q'_i q_j \times \left(2\delta_{ij} - i\epsilon_{ijk}\sigma_k^{(1)}\right)\left(2\delta_{ba} - i\epsilon_{bac}\tau_c^{(1)}\right) = -\left(\frac{M_N^2 g_A h_A^2}{18 f_\pi^3\Delta M}\right)\tau_a^{(2)}(\sigma^{(2)}\cdot\vec{q})\frac{1}{q^2 - m_\pi^2}q'_i q_j \times \left(\left[4\delta_{ij}\delta_{ba} - \epsilon_{ijk}\sigma_k^{(1)}\epsilon_{bac}\tau_c^{(1)}\right] - 2i\left\{\epsilon_{ijk}\sigma_k^{(1)}\delta_{ab} + \delta_{ij}\epsilon_{bac}\tau_c^{(1)}\right\}\right), \tag{B4}$$

$$iA_{(d)} = -\left(\frac{M_N^2 g_A h_A^2}{18 f_\pi^3\Delta M}\right)\tau_a^{(2)}(\sigma^{(2)}\cdot\vec{q})\frac{1}{q^2 - m_\pi^2}q'_i q_j \times \left(2\delta_{ij} - i\epsilon_{jik}\sigma_k^{(1)}\right)\left(2\delta_{ba} - i\epsilon_{abc}\tau_c^{(1)}\right)$$

$$= -\left(\frac{M_N^2 g_A h_A^2}{18 f_\pi^3 \Delta M}\right) \tau_a^{(2)} \left(\sigma^{(2)} \cdot \vec{q}\right) \frac{1}{q^2 - m_\pi^2} q'_i q_j \times \left(\left[4\delta_{ij}\delta_{ba} - \epsilon_{ijk}\sigma_k^{(1)}\epsilon_{bac}\tau_c^{(1)}\right] + 2i\left\{\epsilon_{ijk}\sigma_k^{(1)}\delta_{ab} + \delta_{ij}\epsilon_{bac}\tau_c^{(1)}\right\}\right) \quad \text{(B5)}$$

where in both amplitudes the momentum of the outgoing (virtual) pion is labeled as q' (q). In both amplitudes the terms in [...] exhibit the same spin-isospin structure as the c_i terms discussed above, while those in {...} have a different structure.

Therefore, when Figs. 9(c) and 9(d) are added together, only the structures of the c_i parameters survive. However, due to the above-mentioned selection rules, the diagrams contribute individually to different channels of $NN \to NN\pi$. To be specific, the Fig. 9(d) vanishes for the isospin-1 to isospin-zero transition, i.e., for $pp \to (d/pn_{I=0})\pi^+$, whereas the Fig. 9(c) does not. Furthermore, once the isospin matrix element is evaluated for the Fig. 9(c) it turns out that the expression in {...} gives the same contribution as the one from [...]. The same holds for the isospin-zero to the isospin-1 transition, i.e., for $pn \to pp\pi^-$: Fig. 9(c) does not contribute, whereas the terms in brackets {...} and [...] for Fig. 9(d) are equal. Therefore, in the limit $\Delta M \to \infty$, one indeed observes both properties simultaneously, namely that the $N\Delta$ intermediate state does not contribute if the external NN state is in the isospin-zero state and that the Δ effects can be absorbed in local counter terms, namely c_3 and c_4.

We are now also in the position to see how the pattern changes when we start to move away from the limit $\Delta M \to \infty$. Then the factors $1/\Delta M$ that appear in Eqs. (B1)–(B5) should be replaced by the dynamical $N\Delta$ propagators. One finds for the resulting combination of the propagators for both πN scattering and $NN \to NN\pi$

$$\frac{1}{\Delta M - \omega_\pi} \pm \frac{1}{\Delta M + \omega_\pi}, \quad \text{(B6)}$$

where we used that $\omega_\pi \simeq E_{\rm tot}$ and dropped terms significantly smaller than m_π. In this expression the upper (lower) sign refers to the combination of propagators relevant for the terms that can (cannot) be mapped onto the c_i. Thus, the additional terms are suppressed by

$$\delta = \omega_\pi / \Delta M. \quad \text{(B7)}$$

Numerically δ is already as large as 0.5 at threshold and grows as one goes to higher energies. Clearly, near the two-pion production threshold, $\delta \simeq 1$ and it is necessary to keep the Δ as dynamical degrees of freedom. See Ref. [70] for a power counting that allows one to also study the latter regime.

[1] S. Weinberg, Physica A **96**, 327 (1979).
[2] J. Gasser and H. Leutwyler, Ann. Phys. **158**, 142 (1984).
[3] G. Colangelo, J. Gasser, and H. Leutwyler, Nucl. Phys. **B603**, 125 (2001).
[4] V. Bernard and U.-G. Meißner, Annu. Rev. Nucl. Part. Sci. **57**, 33 (2007).
[5] P. F. Bedaque and U. van Kolck, Annu. Rev. Nucl. Part. Sci. **52**, 339 (2002); E. Epelbaum, Prog. Part. Nucl. Phys. **57**, 654 (2006); E. Epelbaum, H.-W. Hammer, and U.-G. Meißner, arXiv:0811.1338 [nucl-th], Rev. Mod. Phys. (in print).
[6] S. Weinberg, Phys. Lett. **B251**, 288 (1990).
[7] S. Weinberg, Nucl. Phys. **B363**, 3 (1991).
[8] B. Y. Park, F. Myhrer, J. R. Morones, T. Meissner, and K. Kubodera, Phys. Rev. C **53**, 1519 (1996).
[9] C. Hanhart, J. Haidenbauer, M. Hoffmann, U.-G. Meißner, and J. Speth, Phys. Lett. **B424**, 8 (1998).
[10] V. Bernard, N. Kaiser, and U.-G. Meißner, Eur. Phys. J. A **4**, 259 (1999).
[11] V. Dmitrašinović, K. Kubodera, F. Myhrer, and T. Sato, Phys. Lett. **B465**, 43 (1999); S. I. Ando, T. S. Park, and D. P. Min, *ibid.* **B509**, 253 (2001).
[12] T. D. Cohen, J. L. Friar, G. A. Miller, and U. van Kolck, Phys. Rev. C **53**, 2661 (1996).
[13] C. A. da Rocha, G. A. Miller, and U. van Kolck, Phys. Rev. C **61**, 034613 (2000).
[14] C. Hanhart, U. van Kolck, and G. A. Miller, Phys. Rev. Lett. **85**, 2905 (2000).
[15] C. Hanhart and N. Kaiser, Phys. Rev. C **66**, 054005 (2002).
[16] C. Hanhart, Phys. Rep. **397**, 155 (2004).
[17] V. Lensky, V. Baru, J. Haidenbauer, C. Hanhart, A. E. Kudryavtsev, and U.-G. Meißner, Eur. Phys. J. A **27**, 37 (2006).
[18] D. S. Koltun and A. Reitan, Phys. Rev. **141**, 1413 (1966).
[19] C. Hanhart and A. Wirzba, Phys. Lett. **B650**, 354 (2007); Y. Kim, T. Sato, F. Myhrer, and K. Kubodera, Phys. Rev. C **80**, 015206 (2009).
[20] J. A. Niskanen, Nucl. Phys. **A298**, 417 (1978).
[21] C. Hanhart, J. Haidenbauer, O. Krehl, and J. Speth, Phys. Lett. **B444**, 25 (1998).
[22] C. Hanhart, J. Haidenbauer, O. Krehl, and J. Speth, Phys. Rev. C **61**, 064008 (2000).
[23] E. Epelbaum, A. Nogga, W. Glöckle, H. Kamada, Ulf-G. Meißner, and H. Witala, Phys. Rev. C **66**, 064001 (2002).
[24] V. Lensky, V. Baru, J. Haidenbauer, C. Hanhart, A. E. Kudryavtsev, and U.-G. Meißner, Eur. Phys. J. A **26**, 107 (2005).
[25] V. Lensky, V. Baru, E. Epelbaum, C. Hanhart, J. Haidenbauer, A. E. Kudryavtsev, and U.-G. Meißner, Eur. Phys. J. A **33**, 339 (2007).
[26] A. Gårdestig and D. R. Phillips, Phys. Rev. C **73**, 014002 (2006).
[27] A. Gårdestig, Phys. Rev. C **74**, 017001 (2006).
[28] T. S. Park *et al.*, Phys. Rev. C **67**, 055206 (2003).
[29] A. Gårdestig and D. R. Phillips, Phys. Rev. Lett. **96**, 232301 (2006).
[30] D. Gazit, S. Quaglioni, and P. Navratil, Phys. Rev. Lett. **103**, 102502 (2009).
[31] S. X. Nakamura, Phys. Rev. C **77**, 054001 (2008).
[32] M. Goldberger and K. M. Watson, *Collision Theory* (Wiley, New York, 1964).
[33] R. Omnès, Nuovo Cimento **8**, 316 (1958).
[34] A. Gasparyan, J. Haidenbauer, C. Hanhart, and J. Speth, Phys. Rev. C **69**, 034006 (2004); A. Gasparyan, J. Haidenbauer, and C. Hanhart, Phys. Rev. C **72**, 034006 (2005).
[35] C. Hanhart and K. Nakayama, Phys. Lett. **B454**, 176 (1999); for the discussion here especially the appendix given only in arXiv:nucl-th/9809059 is relevant.

[36] R. W. Flammang *et al.*, Phys. Rev. C **58**, 916 (1998).
[37] J. Haidenbauer, K. Holinde, and M. B. Johnson, Phys. Rev. C **48**, 2190 (1993).
[38] T. E. O. Ericson and W. Weise, in *The International Series of Monographs on Physics* (Clarendon, Oxford, UK, 1988), Vol. 74, p. 479.
[39] A. Kacharava *et al.*, "Spin physics from COSY to FAIR," arXiv:nucl-ex/0511028.
[40] C. Ordóñez and U. van Kolck, Phys. Lett. **B291**, 459 (1992); U. van Kolck, Ph.D. thesis, University of Texas, 1993; C. Ordóñez, L. Ray, and U. van Kolck, Phys. Rev. Lett. **72**, 1982 (1994); Phys. Rev. C **53**, 2086 (1996).
[41] V. Bernard, N. Kaiser, and U.-G. Meißner, Int. J. Mod. Phys. E **4**, 193 (1995).
[42] V. Baru, J. Haidenbauer, C. Hanhart, A. E. Kudryavtsev, V. Lensky, and U.-G. Meißner, Proceedings of the 11th International Conference on Meson-Nucleon Physics and the Structure of the Nucleon (MENU 2007), Julich, Germany, 10–14 September 2007, arXiv:0711.2748 [nucl-th].
[43] H. Krebs, E. Epelbaum, and U.-G. Meißner, Eur. Phys. J. A **32**, 127 (2007).
[44] H. Hahn *et al.*, Phys. Rev. Lett. **82**, 2258 (1999).
[45] F. Duncan *et al.*, Phys. Rev. Lett. **80**, 4390 (1998).
[46] M. Daum *et al.*, Eur. Phys. J. C **25**, 55 (2002).
[47] F. Duncan *et al.*, http://authors.aps.org/eprint/files/1998/Feb/aps1998feb19_001/pwa_algorithm.txt.
[48] R. Bilger *et al.*, Nucl. Phys. **A693**, 633 (2001).
[49] S. Abd El-Samad *et al.* (COSY-TOF Collaboration), Eur. Phys. J. A **17**, 595 (2003).
[50] P. Hauser *et al.*, Phys. Rev. C **58**, R1869 (1998).
[51] Th. Strauch *et al.*, Talk given in the International Conference EXA08, September 2008, Vienna, Austria.
[52] Th. Strauch, Ph.D. thesis, Univeristy of Cologne, 2009.
[53] B. G. Ritchie *et al.*, Phys. Rev. C **47**, 21 (1993).
[54] P. Heimberg *et al.*, Phys. Rev. Lett. **77**, 1012 (1996).
[55] M. Drochner *et al.* (GEM Collaboration), Nucl. Phys. **A643**, 55 (1998).
[56] E. Korkmaz *et al.*, Nucl. Phys. **A535**, 637 (1991).
[57] E. L. Mathie *et al.*, Nucl. Phys. **A397**, 469 (1983).
[58] H. O. Meyer *et al.*, Phys. Rev. Lett. **83**, 5439 (1999); H. O. Meyer *et al.*, Phys. Rev. C **63**, 064002 (2001).
[59] P. N. Deepak, J. Haidenbauer, and C. Hanhart, Phys. Rev. C **72**, 024004 (2005).
[60] H. O. Meyer *et al.*, Nucl. Phys. **A539**, 633 (1992).
[61] H. van Haeringen, Nucl. Phys. **A253**, 355 (1975); *Charged-Particle Interactions: Theory and Formulas* (Coulomb Press Leyden, Leiden, 1985).
[62] A. E. Kudryavtsev, B. L. Druzhinin, and V. E. Tarasov, JETP Lett. **63**, 235 (1996) [Pis'ma Zh. Eksp. Teor. Fiz. **63**, 221 (1996)].
[63] V. Bernard, N. Kaiser, and U. G. Meißner, Nucl. Phys. **A615**, 483 (1997).
[64] M. C. M. Rentmeester, R. G. E. Timmermans, and J. J. de Swart, Phys. Rev. C **67**, 044001 (2003).
[65] D. R. Entem and R. Machleidt, arXiv:nucl-th/0303017.
[66] V. Lensky, Ph.D. thesis, University of Bonn, 2007.
[67] C. Hanhart, J. Haidenbauer, A. Reuber, C. Schütz, and J. Speth, Phys. Lett. **B358**, 21 (1995).
[68] V. Baru, A. M. Gasparian, J. Haidenbauer, A. E. Kudryavtsev, and J. Speth, Phys. At. Nucl. **64**, 579 (2001) [Yad. Fiz. **64**, 633 (2001)].
[69] V. Lensky, J. Haidenbauer, C. Hanhart, V. Baru, A. E. Kudryavtsev, and U.-G. Meißner, Int. J. Mod. Phys. A **22**, 591 (2007).
[70] V. Pascalutsa and D. R. Phillips, Phys. Rev. C **67**, 055202 (2003).